Spring tropical cyclones modulate near-surface isotopic compositions of atmospheric water vapour at Kathmandu, Nepal

Niranjan Adhikari[1, 2], Jing Gao[1, 3,*], Aibin Zhao[1], Tianli Xu[1, 4] Manli Chen[1, 3], Xiaowei Niu[1], Tandong Yao[1, 3]

[1] *State Key Laboratory of Tibetan Plateau Earth System, Resources and Environment, Institute of Tibetan Plateau Research, Chinese Academy of Sciences, Beijing 100101, China*

[2] *University of Chinese Academy of Sciences, Beijing 100049, China*

[3] *Lanzhou University, Lanzhou 733000, China*

[4] *Kathmandu Centre for Research and Education,* Chinese Academy of Sciences –*Tribhuvan University, Kirtipur 44613, Kathmandu, Nepal*

* Correspondence to: Jing Gao, E-mail: gaojing@itpcas.ac.cn

Abstract

While westerlies are recognized as a significant moisture transport in Nepal during the pre-monsoon season, precipitation is also attributed to moisture from cyclones originating in the Bay of Bengal (BoB) or the Arabian Sea (AS). Tropical cyclones exhibit negative isotopic values in both precipitation and atmospheric water vapour; however, the factors influencing isotopic fractionation during tropical cyclones remain poorly understood.The Arabian Sea (AS) and the Bay of Bengal (BoB) are the major part of the Indian Ocean where cyclonic activities prevail each year, resulting in extreme precipitation events, particularly during the pre-monsoon season. Despite the significance of cyclones in Nepal, no studies have investigated their impact on the isotopic composition of atmospheric water vapour ($\delta^{18}O_v$, δD_v, and d-excess$_v$). Here, Wwe

present the results of continuous measurements of the isotopic composition of atmospheric water vapour at Kathmandu from 7 May to 7 June 2021 during two pre-monsoon cyclone events;~~,~~ ~~namely~~ cyclone Tauktae formed over the Arabian Sea, and cyclone Yaas formed over the Bay of Bengal. Our study reveals that tropical cyclones originating from the BoB and the AS during the pre-monsoon season modulate isotopic signals of near-surface atmospheric water vapour in Nepal. Comparing conditions before and after, w~~W~~e observed a significant depletion of $\delta^{18}O_v$ and δD_v during both cyclone, ~~- events compared to before and after the cyclone events which was~~ attributed to changes in moisture sources (local vs. marine) ~~-as inferred from backward moisture trajectories. .The outgoing longwave radiation (OLR) and regional precipitation during cyclone events together with the observed correlation between vertical velocity and $\delta^{18}O_v$ showed high moisture convergence and heavy convection at and around the measurement site which caused unusually depleted $\delta^{18}O_v$ during that period. Moisture convergence and convection were stronger during cyclone Yaas which resulted in higher (lower) d-excess$_v$ ($\delta^{18}O_v$), compared to Tauktae, possibly due to strong downdrafts during the cyclone-related rain events which can transport vapour with higher (lower) d-excess$_v$ ($\delta^{18}O_v$) toward the surface. Our study reveals that tropical cyclones that originated from the BoB and the AS modulate isotopic signals of near-surface atmospheric water vapour considerably in Nepal. Hence caution should be made while interpreting the isotopic variability during the non-monsoon season and the effect of cyclones on the isotopic composition of precipitation and atmospheric water vapour~~ Convective activity plays a pivotal role in the variability of $\delta^{18}O_v$ and δD_v during both cyclones, confirmed by the spatial variations of outgoing longwave radiation (OLR) and regional precipitation during both cyclones. We also found a significant negative correlation between $\delta^{18}O_v/\delta D_v$ and rainfall amount along the trajectories during cyclone Tauktae, probably resulting from integrated

upstream processes linked to the earlier Rayleigh distillation of water vapour via rainfall, rather than local rainfall. The decrease in $\delta^{18}O_v/\delta D_v$ during cyclone Yaas is associated with the intensified convection and moisture convergence at the measurement site, while the lower cloud top temperatures (CTT) and lower cloud top pressure (CTP) during intense convection contribute to higher d-excess values at the final stage of cyclone Yaas. This characteristic is missing during cyclone Tauktae. Our results shed light on key processes governing the isotopic composition of atmospheric water vapour at Kathmandu and may have implications for the paleoclimate reconstruction of tropical cyclone activity.

Keywords: Cyclones; Bay of Bengal; Arabian Sea; Isotopic composition of atmospheric water vapour; Convection; Moisture convergence; Kathmandu

1 Introduction

Although the Indian summer monsoon accounts for more than 80 % of annual rainfall in Nepal, agricultural activities also crucially rely on precipitation in the spring season (also known as the pre-monsoon season). Pre-monsoonal rainfall in Nepal is often associated with cyclonic events that provide sufficient moisture for precipitation to support the timely planting of monsoonal crops. Every year, cyclonic events over the North Indian Ocean result in extreme precipitation events, particularly during the pre-monsoon season with less extreme events during the post-monsoon season (Li et al., 2013). Previous studies have suggested that extreme precipitation in Nepal is mostly fuelled by moisture from the Arabian Sea (AS) and the Bay of Bengal (BoB) (Bohlinger et al., 2017; Boschi and Lucarini, 2019). High sea surface temperatures and the westward movement of tropical cyclones formed over the Western Pacific result in cyclones being formed over the BoB and AS (Mohapatra et al., 2016). The number of cyclones in the AS has ~~dramatically~~ increased recently~~in recent years~~ compared to the number of cyclones in the BoB (Pandya et al., 2021). According to the International Best Track Archive for Climate Stewardship (IBTrACS) project, in 2019 three cyclones originated in the BoB and~~while~~ five cyclones originated in the AS. ~~This increase in cyclone frequency in the AS may be~~ D~~d~~ue to a rise in sea surface temperature ~~, which also~~ lengthenings~~s~~ the cyclone decay period (Li and Chakraborty, 2020). Usually, the impact of cyclones formed over the AS is restricted to the nearest coastal regions. However, in recent years this appears to have changed as cyclones are forming back-to-back over the AS and affecting the entire Indian subcontinent including surrounding regions.~~, likely due to AS warming leading to cyclone intensification~~ (Li and Chakraborty, 2020). Cyclone Tauktae ~~has~~ affected the livelihoods of people both near the coast and further inland during the pre-monsoon season of 2021 (Pandya et al., 2021). The impacts of cyclone Yaas after cyclone Tauktae were also felt in Nepal, where it triggered flooding and landslides in several parts of the country (https://floodlist.com/asia/nepal-flood-landslide-may-2021/). As both cyclones hit in short succession, this led to severe agricultural damage in several parts of India at a critical time when farmers were preparing to sow their rice paddies ahead of the monsoon season (https://reliefweb.int/organization/acaps). In Nepal, ~~most of~~ the damage due to Yaas was mostly limited to the Terai regions which experienced intense and continuous rainfall (https://kathmandupost.com/). ~~At the same time, some hilly regions benefited from these cyclone-induced rains, as they created favourable conditions for farmers preparing their~~

Formatted: Font: Not Bold

Formatted: Font: Not Bold

monsoonal crops. Moisture flux associated with cyclones generally extends over a large area and causes moderate to heavy precipitation along the cyclone path and on the nearest land mass (Chan et al., 2022; Rajeev and Mishra, 2022). Thus, Iit is therefore essential to understand the the moisture transport processes of these extreme rainfall events on atmospheric water vapourinfluence of these extreme rainfall events on atmospheric water vapour, which are in turn related to local clouds and surface energy budgets, determining the amount of moisture available to plants.

Atmospheric water vapour is an important constituent of the hydrological cycle and climate system (Saranya et al., 2017), mainly because of its impacts on solar radiation absorption, cloud formation, and atmospheric heating (Noone, 2012). With climate changeglobal warming, the amount of water vapour in the atmosphere is also expected to increase,. This has createdcreating scientific interest in a variety of fields to elucidate the impact of atmospheric water vapour on changing moisture patterns (Hoffmann et al., 2005).

The isotopic composition of atmospheric water vapour ($\delta^{18}O_v$, $\delta D_{v,}$ and d-excess$_v$) contains comprehensive information about the hydrological cycle and the history of moisture exchange (Noone, 2012; Payne et al., 2007; Risi et al., 2008; Worden et al., 2007). Several studies have shown that the isotopic composition of atmospheric water vapour is an effective indicator of cyclone activity (Munksgaard et al., 2015; Sun et al., 2022) including cyclone evolution and structure (Lawrence et al., 2002). The atmospheric water vapour and precipitation associated with tropical cyclones tend to have extremely depleted isotopic compositions compared to monsoonal rain (Chen et al., 2021; Jackisch et al., 2022; Munksgaard et al., 2015; Sánchez-Murillo et al., 2019), which may be due to the high condensation efficiency and substantial fractionation associated with cyclones. A few studies found a systematic depletion of heavy isotopes towards the cyclone eye (Lawrence et al., 2002, 1998; Lawrence and Gedzelman, 1996; Sun et al., 2022; Xu et al., 2019). For example~~instance~~, ~~studying the~~during cyclone Shanshan, ~~on Ishigaki Island, southwest of Japan,~~ Fudeyasu (2008) observed that isotopic depletion in precipitation and water vapour increased radially inward in the cyclone's outer region, likely due to a rainout effect. ~~associated with condensation efficiency and the isotopic exchange between precipitation and water vapour~~. A study conducted in north-eastern Australia during cyclone Ita in April 2014 underlined~~highlighted~~ the role of synoptic-scale meteorological settings in determining the isotopic variability of atmospheric water vapour (Munksgaard et al., 2015). In Fuzhou, China, Xu et al., (2019) reported a significant depletion in typhoon rain $\delta^{18}O$ ~~which was~~ related to the combined effect of large-scale convection, high condensation efficiency, and recycling of isotopically depleted vapour in the rain shield area. Sánchez-Murillo et al., (2019) highlighted the role of convective and stratiform activity as well as precipitation type and amount. ~~as the main controlling factors of precipitation stable isotopes associated with tropical cyclones.~~ The impact of high stratiform fractions and deep convection on isotopic depletion in precipitation during typhoon Lekima was confirmed by Han et al., (2021). ~~These findings clearly demonstrate that the processes that contribute to high-frequency shifts in the isotopic composition of precipitation and atmospheric water vapour during tropical cyclones are still a matter of debate.~~

Although several studies have examined the isotopic variation of event-based precipitation in Nepal (Acharya et al., 2020; Adhikari et al., 2020; Chhetri et al., 2014), there remains a knowledge gap regarding the isotopic response of atmospheric water vapour during cyclone events. ~~Here,~~ W~~w~~e present for the first time the evolution of the isotopic composition of atmospheric water vapour ($\delta^{18}O_v$, δD_v, and d-excess$_v$) in Kathmandu during two pre-monsoon cyclone events. Isotopic data were collected~~provided~~ in 2021, ~~stretching~~ from one week before to one week after the cyclones~~ events~~. Although neither cyclone passed directly over Kathmandu, their remnant vapour produced several days of rainfall that allowed~~over Kathmandu which enabled~~ us to observe changes in the isotopic composition ~~of atmospheric water vapour~~ at high temporal resolutions and ~~to~~ evaluate the cause of such changes at ~~daily and~~ diurnal scales.

2 Data and methods

2.1 Site description

The Kathmandu station lies on the southern slope of the Himalayas ($27^{\circ}42'$ N, $85^{\circ}20'$ E) at an average altitude of about 1400 m above sea level. Based on an 18-year-long record from the Department of Hydrology and Meteorology, Government of Nepal (~~from~~ 2001 to 2018)~~ (Figure 1)~~, this region has an average annual temperature of ~~about~~ 19° C and ~~average annual~~ precipitation amount of 1500 mm, with ~78% of the annual~~most of the~~ rainfall occurring in the monsoon season from ~~(~~June to September~~)~~ (Adhikari et al., 2020). About 16 % of total annual rainfall in Kathmandu occurs in the pre-monsoon season (March to May) with ~~a corresponding mean maximum (minimum)~~ air temperature ranges from 13 to~~of~~ 28° C~~ (13° C)~~ and averaged relative humidity (RH) of 67 %. Advection of the southern branch of westerlies and evaporation from nearby water bodies are the main contributors to pre-monsoonal precipitation (Yu et al., 2015; Chhetri et al., 2014). These arid westerlies, resulted in diminished temperature and relative humidity (RH) within the region while a substantial presence of moisture was observed over extensive areas encompassing the BoB, the AS, India, and surrounding regions including our sampling site during our study period. Figure 1 shows the elevated specific humidity levels averaged between 1000 hPa and 850 hPa throughout the duration of our study period. ~~The total~~

moisture flux (sum of zonal and meridional fluxes) during the pre-monsoon season is low (<60 kg/m/s) as is specific humidity (~6 g/kg), which is associated with transport by westerlies. The region receives about 78 % of its annual rainfall during the monsoon season with associated mean maximum (minimum) air temperature of 29°C (20°C) and RH of about 82 %. Most of the precipitation over Kathmandu during the monsoon period is due to the influx of humid air masses from the BoB. Average post-monsoon (October and November) and winter (December to February) RH is about 80 % and 78 %, respectively, with similar rainfall contributions (3 %) during both seasons. The mean post-monsoon and winter mean maximum (minimum) air temperature is about 25°C (11°C) and 21°C (4°C), respectively.

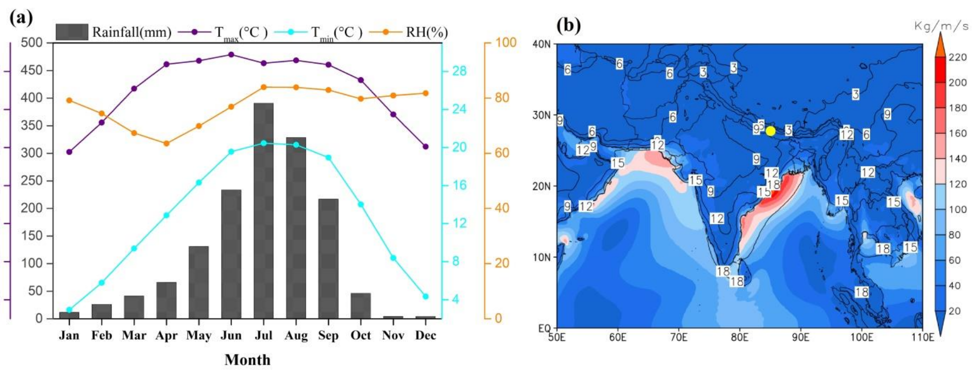

Figure 1 (a) Long-term (2001-2018) average monthly maximum temperatures (T_{max}), minimum temperature (T_{min}), relative humidity (RH), and precipitation amount (P) at Kathmandu. (b) Spatial distribution of long-term (1990-2021) average specific humidity (in g/Kg) (contour lines) and mean vertically integrated moisture flux (colour) during the pre-monsoon season. The yellow dot shows the location of the Kathmandu site.

Formatted: Normal

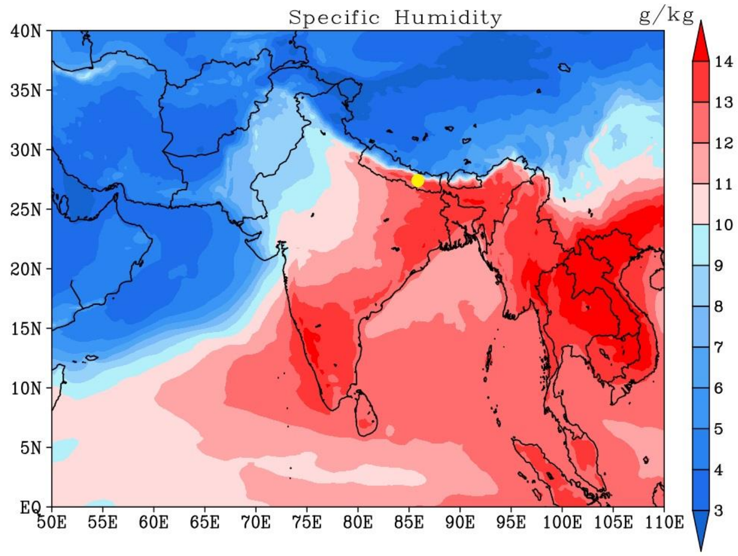

Figure 1 Spatial distribution of specific humidity averaged over 1000 hPa to 850 hPa (in g/Kg) during the period of study. The yellow dot shows the location of Kathmandu.

Formatted: Normal, Centered

Formatted: Normal, Centered

2.2 The evolution of cyclones Tauktae and Yaas and weather conditions at Kathmandu

Cyclone Tauktae developed as a tropical disturbance on 13 May 2021 over the AS, ~~and had~~ evolved into a deep depression by 14 May, moved~~ing~~ north, ~~ward~~ and gradually intensifying ~~over the warm coastal water~~ before turning into a cyclonic storm with wind speeds reaching 75 km/h on that same day (Pandya et al., 2021). ~~Even~~ A~~a~~fter making landfall in the Gir-Somnath district of Gujarat, Tauktae continued to strengthen and was classified as an extremely severe cyclonic storm on 17 May reaching maximum wind speeds of 220 km/h ~~as per the Indian Meteorological Department's Tropical Cyclone Intensity Scale~~ (Verma and Gupta, 2021; Pandya et al., 2021). Cyclone weakened into a low depression on 18 May 2021 at 17:00 h Indian Local

Time (ILT) and finally dissipated one day later. Due to its large convective area, it brought heavy rainfall to different regions of India and Nepal.

The signal of cyclone Tauktae was first detected at the Kathmandu site on 19 May at approximately 03:00 local time (LT), followed by light drizzle. The recorded air temperature was about 22°C, and the relative humidity (RH) was approximately 72%. Within 16 hours, the RH increased from 72% to 91%, while the temperature dropped from 22°C to around 19°C. The maximum RH and minimum temperature were observed on 21 May around 04:00 h LT, reaching 92% and 17°C, respectively.

Cyclone Yaas started out as a depression over the BoB on 22 May 2021 at 08:30 h ILT and gradually intensified into a deep depression before turning into a cyclonic storm on 24 May at around 00:00 h ILT as it moved northeast (Paul and Chowdhury, 2021). The corresponding wind speed and central pressure were recorded as ~~about~~ 65 km/h and 990 hPa, respectively. On 24 May ~~at~~ around 18:00 h ILT, it intensified into a severe cyclonic storm with wind speeds ranging from 89 to 117 km/h before becoming a very severe cyclonic storm on 25 May at 12:00 h ILT with wind speeds from ~~about~~ 119 km/h to 165 km/h. It made landfall north of Odisha on 26 May with maximum sustained wind speeds of 130 km/h to 140 km/h and progressively weakened into a depression on 27 May before~~and~~ dissipating~~ed~~ over northern India on 28 May.

The Kathmandu weather station recorded a total of 59.6 mm of precipitation during cyclone Yaas. Intermittent small patches of rainfall commenced on 25 May at 11:00h LT. The main cyclone event occurred from 26 May at 01:00h LT to 29 May at 01:00h LT. Throughout this period, the ground-level RH fluctuated between 84% and 93%, while surface temperature varied between 18°C and 22°C. Notably, all RH values exceeded 80% from 25 May around 22:00 h LT to 29 May at 10:00 h LT.

Wind speeds, pressure, and cyclone eye location information (3-hour resolution) were taken from datasets of the International Best Track Archive for Climate Stewardship (IBTrACS) project (Knapp et al., 2010), https://www.ncei.noaa.gov/products/). The latter was used to calculate the spatial distance between the cyclone's eye and our measurement location. Figure 2 illustrates the intensity and cumulative rainfall along the paths of the cyclones. A characteristic of both cyclones is the occurrence of rainout along their trajectories, persisting as they move inland.

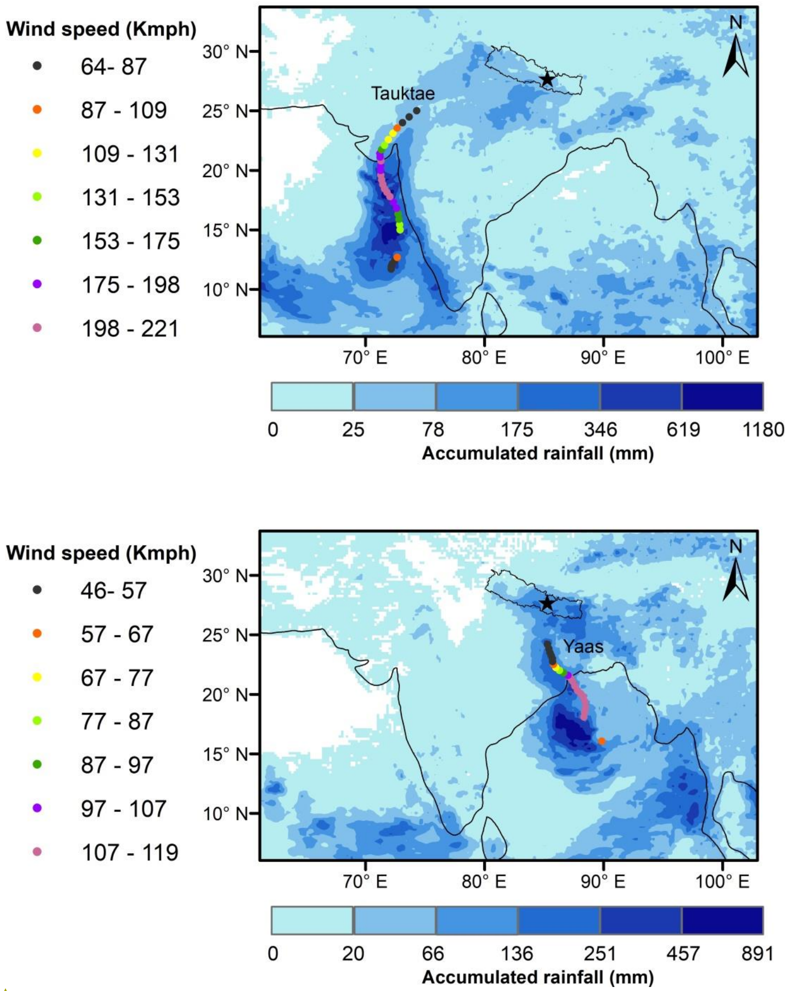

Figure 2 The intensity and track of cyclone Tauktae (Upper panel) and Yaas (Bottom panel) along with accumulated rainfall during their occurrence.

Formatted: Font: Not Bold

Formatted: English (U.S.)

2.3 Isotope measurements ~~and meteorological data~~

Near-surface $\delta^{18}O_v$ and δD_v were measured continuously using a Picarro L2130-i analyser based on wavelength-scanned cavity ring-down spectroscopy (WS-CRDS) (Brand et al., 2009), located at the Kathmandu Centre for Research and Education (KCRE), ~~established by the Chinese Academy of Sciences with the collaboration of Tribhuvan University,~~ Nepal. The sampling inlet consisting of a heated copper tube mounted 7 m above the ground protected with a plastic hood and a 10 L min^{-1} pump transported the sample from the inlet to the analyser.~~An inlet of water vapour was placed 7 m above the grass-covered ground. The copper tube is heated using a self-regulating heat trace isolated with armaflex. To prevent rain from being sucked into the tube, the head of the inlet was covered with a plastic hood. A 10 L min^{-1} pump quickly transported the vapour from the inlet to the analyser~~. The automated standard delivery module (SDM) was used for ~~standard~~ calibration~~.~~, with each calibration made using two reference standards calibrated against Vienna Standard Mean Ocean Water (VSMOW), covering the isotopic ranges of ambient water vapour at Kathmandu.~~Each calibration was made with two reference standards that had been calibrated against Vienna Standard Mean Ocean Water (VSMOW) covering the isotopic ranges of ambient water vapour at Kathmandu.~~ Each reference standard was measured continuously for a total of 75 min each day at three different humidity levels (25 min per level). The dry air passed through Drierite™ desiccant (Merck, Germany) and was delivered to the Picarro analyser for standard measurements. ~~The evaporated standard was then mixed with dry air obtained via Drierite™ desiccant (Merck, Germany) and finally delivered to the Picarro analyser for isotopic measurements.~~ The isotopic composition of atmospheric water vapour is reported as parts per thousand (‰) relative to VSMOW using

$$\boldsymbol{\delta^* = (R_A / R_S - 1) \times 1000\ [‰],} \quad \textbf{(1)}$$

where δ^* represents either δD_v or $\delta^{18}O_v$, and R_A and R_S denote the ratios of heavy to light isotopes ($^{18}O/^{16}O$ or D/H) in the sample and standard, respectively (Kendall & Caldwell, 1998; Yoshimura, 2015). As suggested by Dansgaard, (1964), deuterium excess (d-excess$_v$= δD_v-8×$\delta^{18}O_v$) is used as a tracer for moisture source conditions (Liu et al., 2008; Tian et al., 2001). We examinedpresented the hourly isotopic composition of atmospheric water vapour between 7 May and 7 June 2021, covering the Tauktae and Yaas cyclone events (see previous section) including one1 week on either side of the events. An automated weather station (AWS) continuously measured air temperature, relative humidity, dew point temperature, wind speed and direction, rainfall amount, surface pressure, etc. at a sampling rate of 1 min^{-1}.

2.4 Cyclone track data

The International Best Track Archive for Climate Stewardship (IBTrACS) project containing best track datasets of recent and historical tropical cyclones was used to obtain the cyclone track data for this study (Knapp et al., 2010). We downloaded wind speeds, pressure, and cyclone eye location information (3-hour resolution) from https://www.ncei.noaa.gov/products/. The latter was used to calculate the spatial distance between the cyclone's eye and our measurement location.

2.52.4 Meteorological dataSatellite precipitation and Outgoing Longwave Radiation data

An automated weather station (AWS, Davis Vantage Pro2) continuously measured air temperature, relative humidity, dew point temperature, wind speed and direction, rainfall amount, surface pressure, etc. at one-minute intervals from 7 May to 7 June 2021.

We used Integrated Multi-satellite Retrievals for GPM (IMERG) from the Global Precipitation Measurement (GPM) program with a spatial resolution of 0.1° latitude and longitude (Huffman et al., 2017) to analyse the regional rainfall intensity before, during, and after the cyclone events.~~,~~ ~~following a previously reported method (Huffman et al., 2017)~~. These high-resolution ~~IMERG~~ data allow for the identification of convective rainfall areas and the passage of tropical cyclones (Jackisch et al., 2022). They~~and~~ have been used previously to depict cyclone tracks and associated rainfall intensities (Gaona et al., 2018; Jackisch et al., 2022; Villarini et al., 2011).

We further obtained~~For~~ outgoing longwave radiation (OLR), zonal and meridional wind, specific humidity, vertical velocity, pressure, and distribution of relative humidity and temperature data from ERA5 datasets (Herbash et al., 2020) with a spatial resolution of 0.25° from longitude-latitude grids (https://cds.climate.copernicus.eu/). Additionally, we used cloud-top pressure (CTP) and cloud-top temperature (CTT) data from MERRA-2 Reanalysis datasets retrieved from https://giovanni.gsfc.nasa.gov/, with a spatial resolution of 0.5°×0.625°, as indicators of convective intensity.

~~we used the National Centers for Environmental Prediction (NCEP) daily reanalysis of datasets, with a spatial precision of 2.5° from longitude-latitude grids (available at https://www.esrl.noaa.gov/psd/ (Kleist et al., 2009). OLR data has already been used as an index of tropical convection (Liebmann and Smith, 1996). We further obtained zonal and meridional wind, specific humidity, vertical velocity, vertical pressure, and vertical distribution of relative humidity and temperature data from ERA5 datasets with a spatial resolution of 0.25° from longitude-latitude grids (https://cds.climate.copernicus~~.~~eu/).~~

2.62.5 Moisture backward trajectory analysis

To assess the influence of moisture transport history on the isotopic composition of atmospheric water vapour before, during, and after the cyclone events, we analysed five5-day moisture backward trajectories that terminated at the sampling site using the Hybrid Single-Particle Lagrangian Integrated Trajectory (HYSPLIT) model (Draxler and Hess, 1997). The Global Data Assimilation System (GDAS) with a spatial resolution of 1° (Kleist et al., 2009) was used to provide the meteorological forcing for the HYSPLIT model. Variations in specific humidity along the moisture trajectories were also calculated. Considering the variation in boundary layer height at Kathmandu during the study period, ranging from approximately 100 m to 1170 m, and with the majority of the data falling below 600 m, we set the initial starting height for the moisture backward trajectories to 500 m above ground.Since most of the atmospheric vapour is contained within the bottom 2 km, we set the initial starting height for the moisture backward trajectories to 500 m above ground. Additionally, using ERA5 datasets, we determined the average boundary layer height at Kathmandu during the study period as about 620 m, which confirms 500 m as an appropriate choice for the initial starting height to derive the moisture trajectories.

3 Results ~~and discussion~~

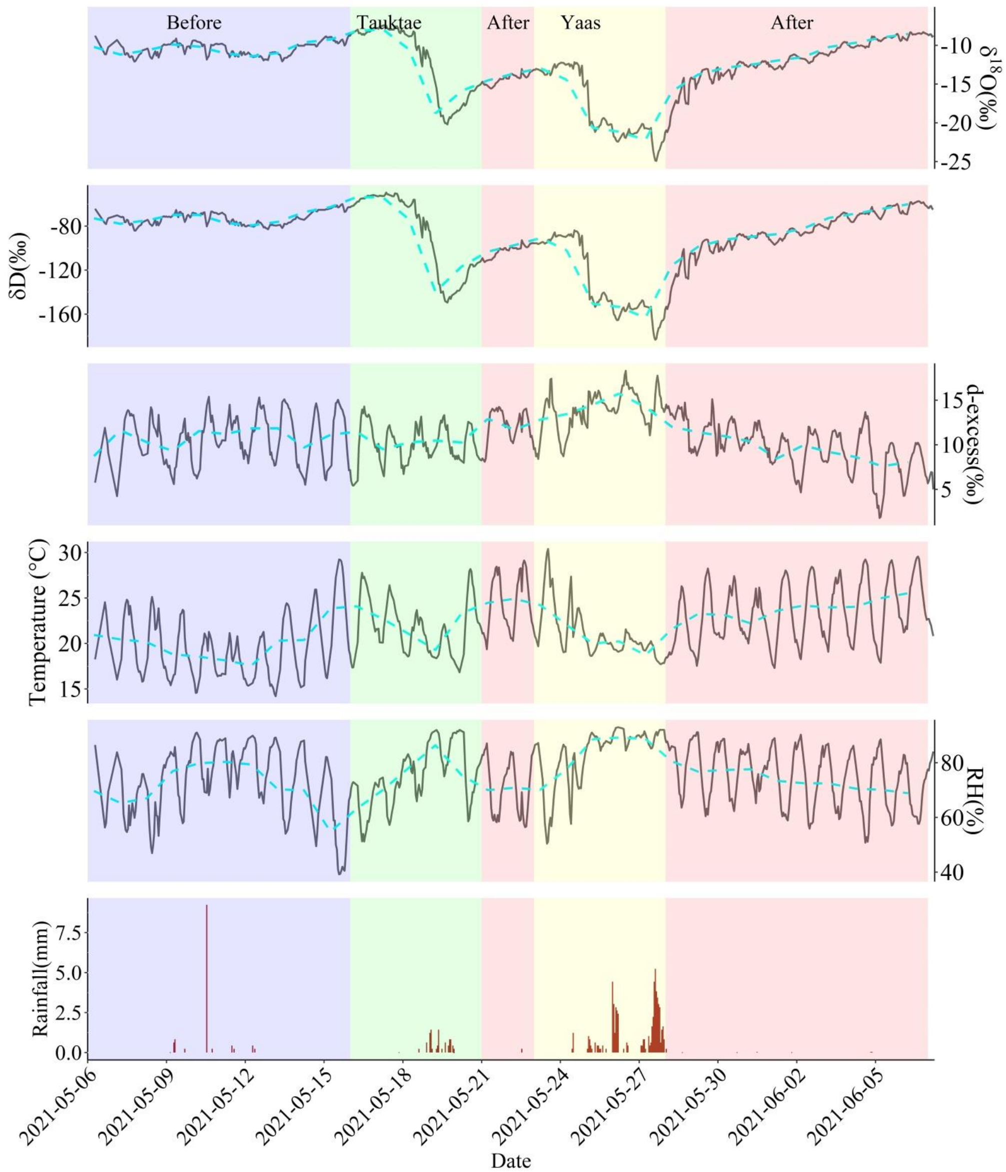

Figure 3 Water vapour isotopic evolution (hourly averages) before, during, and after the

311 Tauktae and Yaas cyclone events along with associated surface air temperature, relative

312 humidity (RH), and rainfall amount. The cyan dashed line represents daily variations.

313 3.1 Water vapour isotope evolution before, during, and after cyclone events

Formatted: Font: Not Bold

314 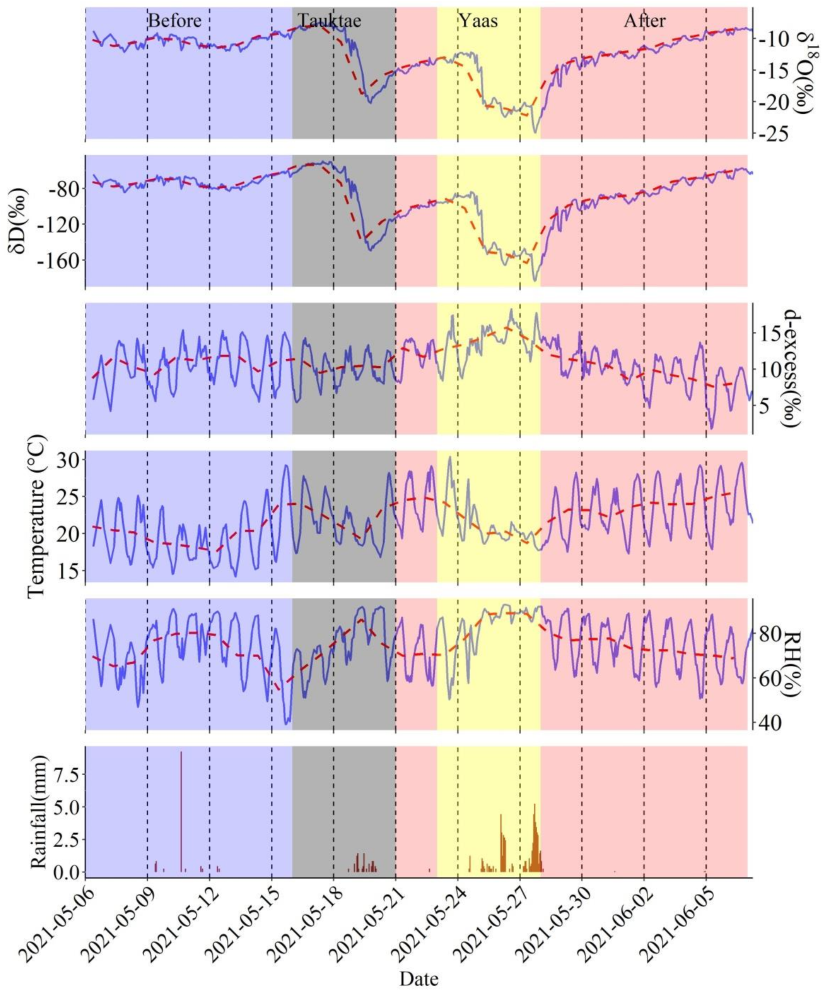

315 Figure 2 Water vapour isotopic evolution (hourly averages) before, during, and after the

316 Tauktae and Yaas cyclone events along with associated surface air temperature, relative

humidity (RH), and rainfall amount. The red dashed line in the figure represents daily variations.

Significant variability was observed in isotopic composition before, during, and after the cyclones at Kathmandu station (and Table 1). $\delta^{18}O_v$ and δD_v showed a sudden depletion in the final stages of both cyclones, coinciding with RH reaching maximum values. The depletion was more pronounced during cyclone Yaas compared to cyclone Tauktae.

Formatted: English (U.S.)

The isotopic composition of atmospheric water vapour surrounding the two cyclone events shows significant variability at Kathmandu station (Figure 2, Table 1). $\delta^{18}O_v$ and δD_v showed a sudden depletion in the final stages of both cyclones, which coincides with RH reaching its maximum values. The depletion was more pronounced during cyclone Yaas compared to cyclone Tauktae. Before the cyclone Tauktae, $\delta^{18}O_v$ (δD_v) varied from -7.40 ‰ (-49.53 ‰) to -12.10 ‰ (-84.15 ‰) with an average of -10.04 ‰ (-69.51 ‰) and d-excess$_v$ ranged from 4.24 ‰ to 15.38 ‰ with an average of 10.84 ‰.Before the cyclone Tauktae, $\delta^{18}O_v$ (δD_v) varied from -8.38 ‰ (-60.10 ‰) to -12.10 ‰ (-84.15 ‰) with an average of -10.52 ‰ (-73.22 ‰) and d-excess$_v$ ranged from 4.24 ‰ to 15.28 ‰ with an average of 10.94 ‰. The highest $\delta^{18}O_v$ value of -7.40 ‰ was observed before the cyclone Tauktae, whereas the lowest $\delta^{18}O_v$ value of -24.92 ‰ was observed during the final stages of cyclone Yaas. Clearly, TThe isotopic composition of atmospheric water vapourclearly shows a downward trend as the remnant of cyclones passed over Kathmandu. $\delta^{18}O_v$ decreased by over 12 ‰ from 14 May to 20 May (Tauktae) and again between 24 May and 29 May (Yaas), reaching minima for $\delta^{18}O_v$ (δD_v) of -20.21 ‰ (-149.49 ‰) and -24.92 ‰ (-183.34 ‰), respectively. During Tauktae, $\delta^{18}O_v$ (δD_v) varied from -8.20‰ (-56.06‰) to -20.21‰ (-149.49‰) with an average of -14.73‰ (-106.76‰) and during Yaas $\delta^{18}O_v$ (δD_v) ranges from -12.17‰ (-83.85‰) to -24.92‰ (-183.34‰) with an average of -17.87‰ (-129.18‰). Similarly, d-excess$_v$ during Tauktae varied from 7.97 ‰ to 14.24 ‰ with an average of 11.06 ‰ while during Yaas it varied from 8.71 ‰ to 18.29 ‰ with an average of 13.77 ‰. After both cyclones had dissipated, $\delta^{18}O_v$ (and δD_v) started to recover pre-cyclone values of -8.29 ‰ to -14.94 ‰ (-57.40 ‰ to -109.31 ‰), with an average of -11.09 ‰ (-79.38 ‰), and d-excess ranged between 1.80 ‰ and 15.11 ‰ with an average of 9.37 ‰. ~~During Tauktae, d-excess$_v$ varied from 6.47 ‰ to 18.79 ‰ with an average of 10.87 ‰ while during Yaas it varied from 8.71 ‰ to 18.29 ‰ with an average of 13.77 ‰. After both cyclones had dissipated, $\delta^{18}O_v$ (and δD_v) started to recover pre-cyclone values of -8.29 ‰ to -14.94 ‰ (-57.40 ‰ to -109.31 ‰), with an average of -11.09 ‰ (-79.38 ‰). During that period, d-excess ranged between 1.80 ‰ and 15.11 ‰ with an average of 9.37 ‰. Notably, the isotopic composition of atmospheric water vapour before the commencement of rainfall by Tauktae remained enriched, suggesting that the isotopic composition of atmospheric vapour during that period was representative of surface layer inflow (Munksgaard et al., 2015). However, $\delta^{18}O_v$ and δD_v at the earlier stage of cyclone Yaas were significantly lower as compared to the earlier stage of cyclone Tauktae. These discrepancies might be due to the timing of their occurrence or the convective strength.~~

The remnants of cyclone Tauktae caused light rain at Kathmandu, with a significant depletion in $\delta^{18}O_v$ (δD_v) by ~8 ‰ (~66 ‰) on 20 May compared to the previous day. From the formation of a depression over the AS on 14 May 2021 until the dissipation inland on 19 May (Fig. S3), no significant variation in the isotopic composition in atmospheric water vapour at Kathmandu was observed (Fig. 3). After the dissipation, when the residual Tauktae vapour passed the Kathmandu site producing light rains, $\delta^{18}O_v$ and δD_v began to decrease independently of the rainfall amount, starting on 19 May around 11:00 h Local Time (LT), from -8.34 ‰ for

$\delta^{18}O_v$ and -56.06 ‰ for δD_v and decreasing in one hour to -10.12 ‰ and -68.41 ‰ respectively. This decrease continued for 24 hours reaching a minimum of -20.21 ‰ and -149.49 ‰ for $\delta^{18}O_v$ and δD_v respectively on 20 May at 12:00 h LT. However, d-excess$_v$ did not show notable variations during the passage of cyclone Tauktae. $\delta^{18}O_v$ and δD_v remained depleted from 20 to 22 May.

On 24 May, cyclone Yaas formed over the BoB and followed a trajectory through north-eastern India (Fig. S4). The effect of cyclone Yaas on $\delta^{18}O_v$ and δD_v at Kathmandu was observed on 25 May with $\delta^{18}O_v$ (δD_v) dropping rapidly from -12.62 ‰ (-88.71 ‰) on 25 May at 20:00 h LT to -15.07 ‰ (-106.22 ‰) just one hour later. At the same time, d-excess$_v$ increased from 12.30 ‰ to 14.34 ‰. The depletion continued until 28 May with a minimum of $\delta^{18}O_v$ (δD_v) by -24.92 ‰ (-182.35 ‰) at 16:00 h LT. Yaas had already weakened into a low-pressure area over Bihar in south-eastern Uttar Pradesh, India. $\delta^{18}O_v$ and δD_v started to increase by about 10 ‰ on 29 May at 16:00 h LT after Yaas had dissipated. From 25 to 29 May, d-excess$_v$ gradually increased as opposed to $\delta^{18}O_v$ and δD_v, resulting in a negative correlation with $\delta^{18}O_v$ and δD_v of -0.60 and -0.55 respectively.

The passage of cyclones that had formed over the AS (Tauktae) and BoB (Yaas) caused significant depletion in the isotopic composition of atmospheric ~~water vapour~~ and led to cumulative rainfall of 9.2 mm (Tauktae) between 14 May and 20 May 2021 and 59.6 mm (Yaas) between 25 May and 28 May 2021 at our site. This depletion is due to ~~This is in agreement with previous studies which documented similar depletion in isotope ratios due to~~ cyclone-associated intense rainfall and agrees with previous studies (Krishnamurthy and Shukla, 2007; Rahul et al., 2016). ~~It is noteworthy that~~Note the above $\delta^{18}O_v$ minimum observed during cyclone Yaas is similar to the minimum observed in Bangalore, India ($\delta^{18}O_v$ =-22.5 ‰) (Rahul et al., 2016) and

Roorkee, India ($\delta^{18}O_v$ =-25.35 ‰) (Saranya et al., 2018) when cyclones evolved over the BoB, ~~were closest to~~passed near their sampling sites. These results indicate a similar oceanic source of moisture during cyclones. We discuss the influence of moisture sources in Sect. 4.1. ~~indicate the significant impact of oceanic moisture on the isotopic composition of atmospheric water vapour over the continental during the time of cyclones. We will discuss the influence of moisture sources in Sect. 3.3 in more detail.~~

The relation between $\delta^{18}O_v$ and δD_v varies for the periods before, during, and after the cyclones, showing different slopes and intercepts with the Local Meteoric Vapour Line (LMVL) (Fig. 4~~Figure 3~~). Before the first ~~cyclone~~ event, both the slope (5.85) and intercept (-12.12) are significantly lower ~~(slope=5.85 and intercept= -12.12)~~, indicating the strong influence of non-equilibrium processes such as evaporation. During both cyclones ~~events~~, both the slopes and intercepts resemble ~~the slope and intercept~~those of the global meteoric water line (GMWL: $\delta D=8\times\delta^{18}O+10$) (Figure ~~Figure 3~~). After the cyclone ~~events~~, the slope and intercept decreased to 7.37 and to 2.34, respectively, ~~which~~ implying~~ies~~ a change of moisture sources and evaporation ~~becoming dominant once again~~.

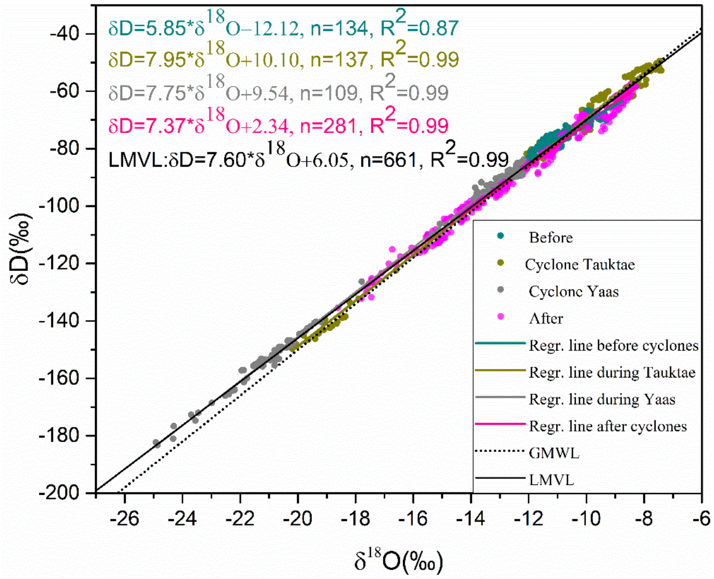

Figure 3 4 Relationships between $\delta^{18}O_v$ and δD_v before, during, and after the cyclone events. The regression lines for each period are presented along with GMWL for comparison.

Table 1 Descriptive statistics of $\delta^{18}O_v$, δD_v, and d-excess$_v$ measured before, during, and after the cyclone events.

Period	$\delta^{18}O_v$ [‰]			δD_v [‰]			d-excess$_v$ [‰]		
	min	max	avg	min	max	avg	min	max	avg
Before	-12.10	-7.40	-10.04	-84.15	-49.53	-69.51	4.24	15.38	10.84
Cyclone Tauktae	-20.21	-8.20	-14.73	-149.49	-56.06	-106.76	7.97	14.24	11.06
Cyclone Yaas	-24.92	-12.17	-17.87	-183.34	-83.85	-129.18	8.71	18.29	13.77
After	-14.94	-8.29	-11.09	-109.31	-57.40	-79.38	1.80	15.11	9.37

To assess the meteorological influence on the isotopic composition at Kathmandu, we examined the linear correlations between the isotopic composition ($\delta^{18}O_v$, δD_v, and d-excess$_v$), and air temperature (T), relative humidity (RH), precipitation amount (P), wind speed (WS), and dew point temperature (T_d) before, during, and after the cyclones (Table 2). Before the cyclones, both $\delta^{18}O_v$ and δD_v showed a positive correlation with air temperature (i.e., temperature effect) and dew point temperature but no correlations with other meteorological variables (Table 2). The correlation between $\delta^{18}O_v$/δD_v and surface air temperature and RH became weaker during the cyclone Tauktae while much stronger (r=0.60 for temperature and r=-0.68 for RH) during Yaas. During Tauktae, we did not observe any effect of precipitation amount on the isotopic composition, while during Yaas there was a negative correlation (r=-0.56). D-excess$_v$ was positively correlated with local air temperature (negatively correlated with local RH) before, during, and after Tauktae, whilst no correlations were observed during Yaas (Table 2).

Table 2 Linear correlations between the isotopic composition of atmospheric water vapour ($\delta^{18}O_v$, δD_v, and d-excess$_v$) and air temperature (T), relative humidity (RH), precipitation amount (P), wind speed (WS), and dew point temperature (T_d) before, during, and after the cyclone events. *, **, and * indicate correlation significance levels of 0.001, 0.01, and 0.05 respectively.**

	T	RH	P	WS	T_d
Before					
$\delta^{18}O_v$	0.24***	-0.03	-0.41	-0.10	0.51***
δD_v	0.44***	0.21**	-0.37	0.08	0.63***
d-excess$_v$	0.66***	-0.64***	0.35	0.68***	0.28***
Cyclone Tauktae					
$\delta^{18}O_v$	0.15	-0.19	0.11	-0.004	0.07
δD_v	0.21*	-0.25**	0.10	0.05	0.11
d-excess$_v$	0.77***	-0.82***	-0.22	0.61***	0.51***
Cyclone Yaas					
$\delta^{18}O_v$	0.60***	-0.68***	-0.56***	0.02	0.23**
δD_v	0.63***	-0.70***	-0.56***	0.05	0.26**
d-excess$_v$	0.10	-0.006	0.19	0.32**	0.26*
After					
$\delta^{18}O_v$	0.17*	-0.19*	-	0.19*	0.09
δD_v	0.30***	-0.31***	-	0.30***	0.20*
d-excess$_v$	0.62***	-0.58***	-	0.52***	0.55***

3.2 Day-to-day and diurnal variations during cyclones events

To understand the depletions in $\delta^{18}O_v$ and δD_v during the Tauktae and Yaas cyclone events, we analysed the regional wind fields and specific humidity over the Northern Indian Ocean during the respective periods. Fig. S3 shows the genesis, development, movement, and dissipation of cyclone Tauktae together with changes in specific humidity along the transport path. The remnants of cyclone Tauktae caused light rain at Kathmandu, with a significant depletion in $\delta^{18}O_v$ (δD_v) by ~8 ‰ (~66 ‰) on 20 May as compared to the previous day. From the formation of a depression over the AS on 14 May 2021 until the commencing dissipation inland on 19 May, no significant variation in the isotopic composition of atmospheric water vapour was observed (Fig. 2). After the dissipation, when the residual Tauktae vapour passed the Kathmandu producing light rains, $\delta^{18}O_v$ and δD_v began to decrease independently of the rainfall amount, starting on 19 May at around 11:00 h Local Time (LT) from -8.34 ‰ for $\delta^{18}O_v$ and -56.06 ‰ for δD_v and dropping in just one hour to -10.12 ‰ and -68.41 ‰ respectively. This decrease continued for another day, reaching a minimum of -20.21 ‰ and -149.49 ‰ for $\delta^{18}O_v$ and δD_v respectively on 20 May at around 12:00 h LT. However, d-excess$_v$ did not show notable variations during the passage of cyclone Tauktae. $\delta^{18}O_v$ and δD_v remained anomalously depleted from 20 to 22 May due to the presence of a remnant of cyclone Tauktae.

On 24 May, cyclone Yaas formed over the BoB and started along a northward trajectory through north-eastern India (Fig. S4). The high specific humidity over India and surrounding regions during the days of cyclone formation indicates that Yaas had lifted a large amount of water vapour from the BoB, which subsequently produced intense rainfall along its path. The effect of cyclone Yaas on $\delta^{18}O_v$ and δD_v at Kathmandu was first captured on 25 May with $\delta^{18}O_v$ (δD_v) dropping rapidly from -12.62 ‰ (-88.71 ‰) on 25 May at 20:00 h LT to -15.07 ‰ (-106.22 ‰) just one hour later. At the same time, d-excess$_v$ was increased from 12.30 ‰ to 14.34 ‰. The depletion continued until 28 May with a minimum of $\delta^{18}O_v$ (δD_v) by -24.92 ‰ (-182.35 ‰) at 16:00 h LT. At that time, Yaas had already weakened into a low-pressure area over Bihar in south-eastern Uttar Pradesh, India. $\delta^{18}O_v$ and δD_v started to increase after Yaas had dissipated, reaching -14.64 ‰ for $\delta^{18}O_v$ and -103.97 ‰ for δD_v on 29 May at 16:00 h LT. From 25 to 29 May, d-excess$_v$ gradually increased, resulting in a strong negative association with $\delta^{18}O_v$ and δD_v, with correlation coefficients of -0.60 and -0.55 respectively. Such strong isotopic depletion during cyclone events might be associated with high condensation efficiencies within the cyclones leading to extensive fractionation (Rahul et al., 2016).

To further elucidate the processes affecting the diurnal variability of the isotopic composition of atmospheric water vapour, we investigated the mean diurnal cycles of $\delta^{18}O_v$, δD_v, d-excess$_v$, surface temperature, and specific humidity during the cyclone events, focussing on the last 4 days of each cyclone (19 May to 22 May for Tauktae and 25 May to 28 May for Yaas) when the measurement site received the first precipitation caused by cyclones. Surprisingly, we observed very weak diurnal signals in $\delta^{18}O_v$ and δD_v during either cyclone event (Figure 4), with amplitudes of diurnal variations in $\delta^{18}O_v$ (δD_v) of 1.10 ‰ (10.21 ‰) during cyclone Tauktae and 2.06 ‰ (16.07 ‰) during cyclone Yaas. The surface temperature and specific humidity showed an average peak-to-peak variability of about 7 °C and 2 g/kg, respectively, during the cyclone Tauktae. In contrast, these values were considerably lower during Yaas with respective peak-to-peak variabilities of about 3 °C and 0.94 g/kg. Unlike $\delta^{18}O_v$ and δD_v, d-excess$_v$ showed a clear diurnal pattern consisting of a gradual increase from early morning till about midday, followed by about 4:00 h during which d-excess remained at a high level, before starting to gradually decrease from about 16:00 h onward (Figure 4). This diurnal variation in d-excess$_v$ seems to have been more prominent during cyclone Tauktae with a peak-to-peak variability of 3.87 ‰ (vs 1.90 ‰ during cyclone Yaas). The d-excess$_v$ diurnal cycle during Tauktae was strongly synchronized with surface temperature and specific humidity with respective correlation coefficients (R^2) of 0.96 and 0.81. During Yaas, the synchronicity was considerably weaker exhibiting correlation coefficients (R^2) of 0.27 and 0.35 with temperature and specific humidity, respectively. Considering that rather smaller precipitation amount during Tauktae compared to Yaas, neither $\delta^{18}O_v$ nor δD_v showed any notable diurnal signal during these events, indicating that any diurnal variation in $\delta^{18}O_v$ or δD_v during the cyclones events was independent of the day-night variation in local weather parameters and the Rayleigh fractionation processes they underwent during their northward movement (see Sect. 3.3 for a more detailed discussion); whereas local weather parameters may play pronounced roles on d-excess$_v$ diurnal variations depending on rainfall strength.

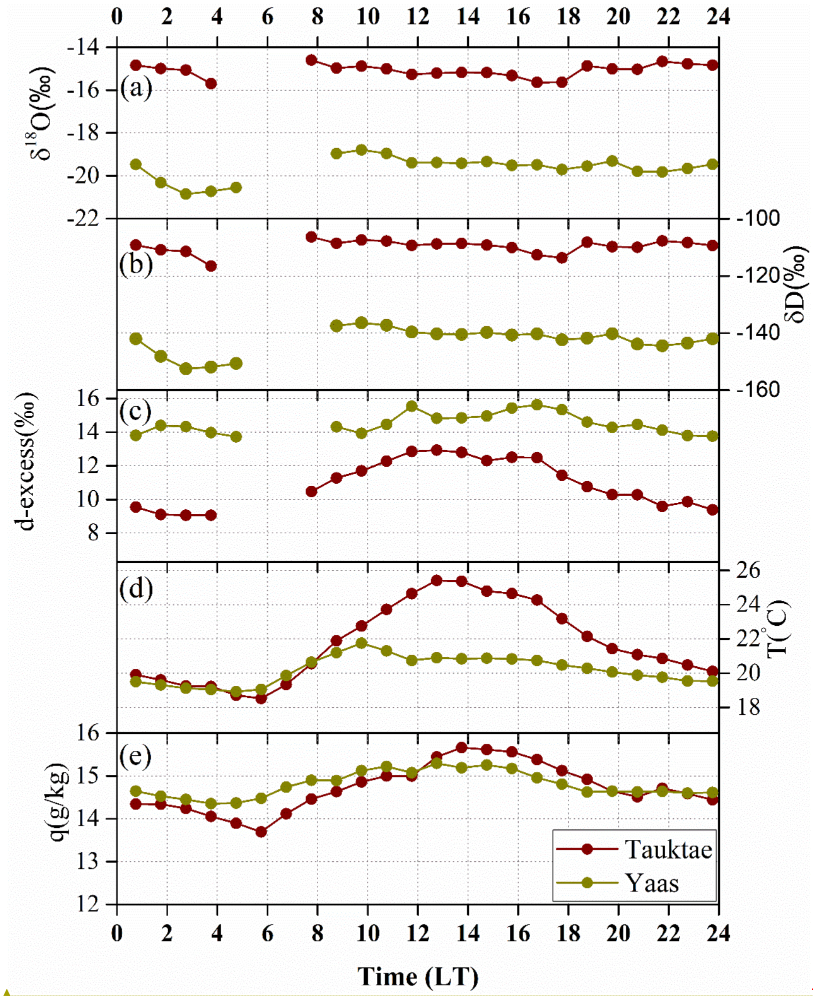

Formatted: Font: Not Bold

Figure 4 Diurnal cycles of (a) $\delta^{18}O_v$, (b) δD_v, (c) d-excess$_v$, (d) temperature (T), and (e) specific humidity (q) averaged from 19 to 22 May during Tauktae and from 25 to 28 May during Yaas. The units of Time "LT" indicates Local Time.

4 Discussions

To investigate the underlying factors behind the isotopic variations, we focused on the impact of moisture sources, by calculating five-day back trajectories for each day before, during, and after the cyclone events and changes of corresponding specific humidity. In addition, we explored the effects of convective activity, moisture convergence, and total rainfall along the back trajectories on water vapour isotopic depletion.

4.1 Influence of Moisture source

3.3 Isotopic response to regional climate

Previous studies suggested that Kathmandu is predominantly impacted by local moisture sources with short and long-range transport of westerlies before the onset of summer monsoon, which is generally dry and characterized by sporadic rainfall with enriched $\delta^{18}O$ values in precipitation (Adhikari et al., 2020; Chhetri et al., 2014; Yu et al., 2016). We now probe the underlying reasons for these isotopic variations in more detail. For this purpose, we analysed the influence of moisture sources on the isotopic composition of atmospheric water vapour by calculating 5-day backward trajectories for each day before, during, and after the cyclone events. We also calculated the associated specific humidity along the cyclone trajectories to estimate moisture uptake and identify possible rainfall regions (Figure 5).

We found significant proportions of moisture trajectories prior to cyclone Tauktae either originated locally or by westerlies, characterized by low specific humidity (Fig. 5, upper left panel). These moisture trajectories were traced back to the Gangetic plain before cyclone Tauktae. The associated $\delta^{18}O_v$ and δD_v values for these moisture sources exhibited enrichment,

Formatted: Indent: First line: 0"

with average values of -10.04‰ and -69.51‰ for $\delta^{18}O_v$ and δD_v, respectively. A similar slope (5.85) and intercept (-12.12) of the local meteoric vapour line before Tauktae to the surface water line calculated in the Gangetic plain (Hassenruck‐Gudipati et al., 2023) which provided corroboration for the impact of local evaporation on the isotopic composition. Before the cyclone events, the majority of moisture trajectories associated with high $\delta^{18}O_v$ and δD_v originated either locally or were brought in by westerlies with low specific humidity along their paths. During Tauktae, most trajectories originate in the AS. During Yaas, most trajectories point to the BoB as the sole vapour source contributing to the moisture at the sampling site (Figure 5).

As cyclone Tauktae approached the continent, the primary moisture source at Kathmandu transitioned from local origins to majority AS vapour (Fig. 5, upper right panel). The specific humidity along these trajectories exhibited higher levels over the oceans, diminishing as they traversed over land through precipitation (Fig. 5, upper right panel). During this phase, $\delta^{18}O_v$ and δD_v were significantly lower (on average over 4.5‰ and 37‰ for $\delta^{18}O_v$ and δD_v respectively) than measurements preceding the cyclone. Such depletion can be attributed to the progressive rainout along the moisture transport path, wherein heavy isotopes are removed during successive condensation (Xu et al., 2019). Notably, the isotopic composition before the Tauktae-induced rainfall remained enriched, reflecting inflow from the surface layer (Munksgaard et al., 2015). Furthermore, the d-excess$_v$ variation at Kathmandu during Tauktae may have been influenced by local moisture recycling processes.

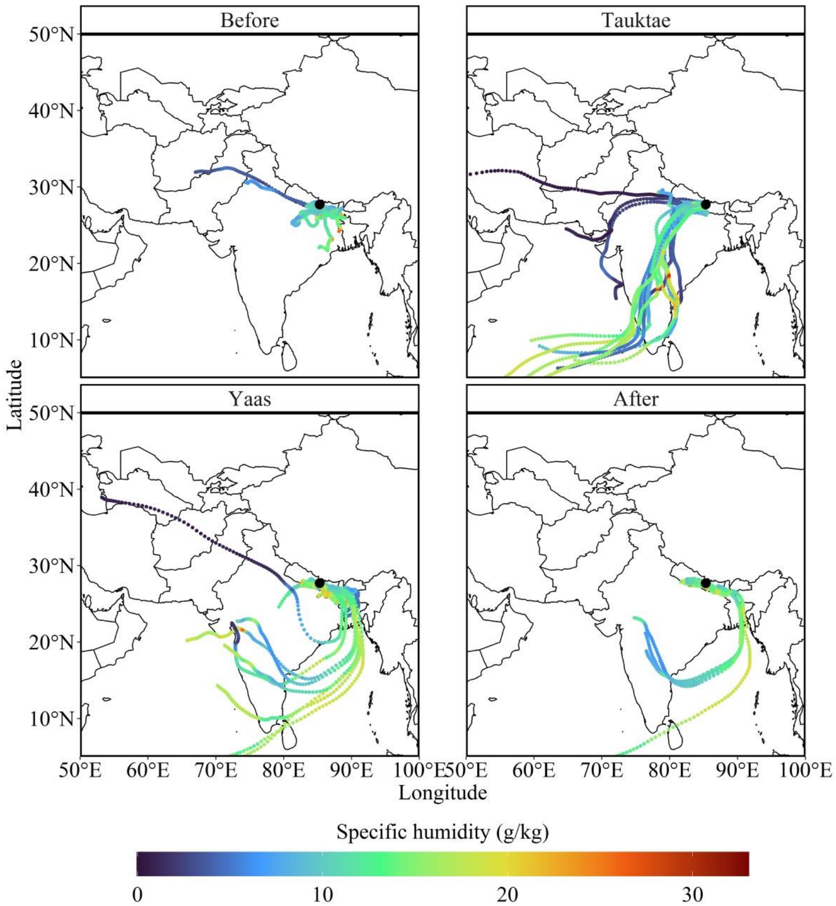

Figure 4 Five-day backward moisture trajectories reaching the sampling site before, during, and after the cyclone events. Colours denote specific humidity (q in g/kg).

During cyclone Yaas, only the BoB vapour contributed to moisture at Kathmandu and specific humidity along the trajectories over the ocean was high (Fig. 5, bottom left panel). The high specific humidity over India and surrounding regions during cyclone formation suggest that Yaas lifted a substantial amount of water vapour from the BoB yielding intense rainfall along its path. The isotopic composition during Yaas was more depleted than that of Tuaktae with averages of -17.87‰ and -129.18‰ for $\delta^{18}O_v$ and δD_v respectively. The difference could stem from varied moisture sources, rainout histories, and the respective strengths of each cyclone. Moreover, the high isotopic depletion during cyclone Yaas might be attributed to the disparity of sea surface water $\delta^{18}O$ between the AS and BoB. The surface water $\delta^{18}O$ in the BoB is relatively depleted compared to the AS (Lekshmy et al., 2014), which results from a substantial influx of freshwater from rain and runoff originating from the Ganga Brahmaputra river basin (Breitenbach et al., 2010; Singh et al., 2010).

Although, the progressive increment was seen in the time series of $\delta^{18}O_v$ and δD_v after the dissipation of Tauktae (Fig. 3), $\delta^{18}O_v$ and δD_v in the earlier stage of Yaas were significantly lower compared to Tauktae because there was not enough time for recovery. There was a strong association between $\delta^{18}O_v$/or δD_v and local meteorological conditions during cyclone Yaas associated with high relative humidity from the remote ocean (Chen et al., 2021; Xu et al., 2019). Furthermore, the negative correlation of $\delta^{18}O_v/\delta D_v$ vs. RH and the fact that $\delta^{18}O_v/\delta D_v$ was depleted highlight the influence of humid moisture sources (Yu et al., 2008), which was also confirmed by our moisture back trajectory analysis (Fig. 5, bottom left panel). A similar correlation was also observed in mid-tropospheric water vapour over the western Pacific associated with intense convective activity (Noone, 2012).

In contrast to cyclone Tauktae, the lack of correlation of d-excess$_v$ with RH and local air temperature during cyclone Yaas implies that local moisture recycling processes are not significant in determining d-excess$_v$ variation and RH might not be a reliable predictor of kinetic fractionation during evaporation. Previous research conducted in the Indian Ocean (e.g., Midhun et al., 2013; Uemura et al., 2008) suggested that the high relative humidity (i.e. >80%) at the sampling sites weakens the correlation between d-excess$_v$ and RH. Our observed data also satisfied that condition during Yaas because the majority of isotopic measurements (about 75%) were associated with high relative humidity (>80%), while this fraction was only 25% during Tauktae.

Following the dissipation of the cyclones, some moisture at Kathmandu was provided by BoB vapour together with local evaporation (Fig. 5, bottom right panel). However, the isotopic composition reverted to the original (enriched) levels ($\delta^{18}O_v$ = -11.09 ‰, δD_v= -79.38 ‰, and d-$excess_v$= 9.37 ‰). The diminished correlation between $\delta^{18}O_v/\delta D_v$ and temperature following the cyclones is attributed to the admixture of vapour originating from plant transpiration during that period (Delattre et al., 2015).

We used the vapour δD_v-q plot combined with the Rayleigh distillation and mixing curve to assess the moisture mixing (Fig. 6). Before the development of cyclone Tauktae and during its early stages, the data points lie well above the mixing curve, indicating that the isotopic variability was mainly dominated by vapour from local evapotranspiration. In contrast, during the latter stage of cyclone Tauktae, δD_v was significantly depleted to levels well below the Rayleigh curve. During the early stage of cyclone Yaas, there are only a few data points between the mixing and Rayleigh curves with the majority well below the Rayleigh curve, particularly during the later stage. During both events, Kathmandu was dominated by deep convection leading to a strong convergence of moisture from both the AS (Tauktae) and the BoB (Yaas). This points towards the influence of convective processes (see Section 4.2) (Galewsky and Samuels-Crow, 2015). After Yaas had dissipated, δD_v gradually increased again with half of the data points clustered between the mixing and Rayleigh curves. The remaining data points were well above the mixing curve, indicating the influence of locally evaporated vapour also evidenced by the moisture back trajectories (bottom right panel).

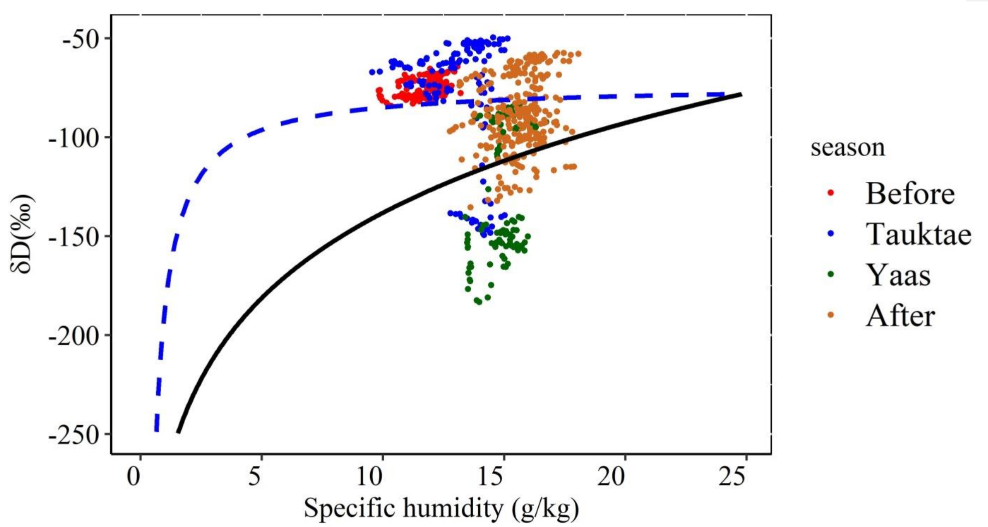

Figure 5 Scatter plot of hourly averaged δD_v vs. specific humidity (q). The solid black curve represents the Rayleigh distillation curve calculated for the initial condition of δD_v =- 78.20 ‰, BoB-averaged δD_v (Lekshmy et al., 2022), SST of 30° C, and RH of 90 %. The dashed blue curve represents the mixing line, calculated based on dry continental air (q= 0.5 g/kg and δD_v =-300 ‰ (Wang et al., 2021)) and the wet source, which corresponds to the initial conditions used to calculate the theoretical Rayleigh curve.

~~Both cyclone events have in common that the specific humidity tends to be high while they are over oceans and the air becomes drier while crossing over land, as moisture is removed through precipitation. We found that the association between both $\delta^{18}O_v$ and δD_v and Temperature/Relative humidity was much stronger during the cyclone events compared to before or after the events (Table 2). This might be linked to the cyclones transporting large amounts of moisture from remote oceans (Chen et al., 2021; Xu et al., 2019). After the cyclones had~~

dissipated, the isotopic composition of atmospheric water vapour reverted to the original (enriched) levels ($\delta^{18}O_v$ = -14.64 ‰, δD_v = -103.97 ‰, and d-excess$_v$ = 13.20 ‰).

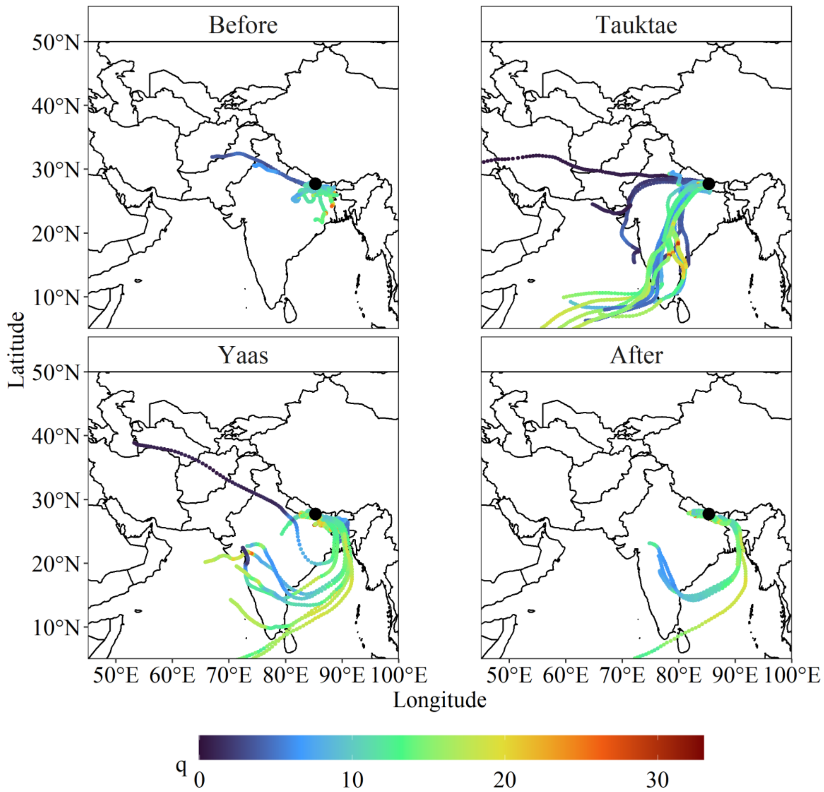

Figure 5 Five-day backward moisture trajectories reaching the sampling site before, during, and after the cyclone events. Colours denote specific humidity (q in g/kg) along the trajectories.

4.2 Influence of deep convection associated with cyclones

Formatted: Font: 14 pt, Bold

One of the most likely causes for large isotopic depletion during cycloness events might be the associated convectiveon processes. Several studies have demonstrated that convective processes within tropical cyclones can cause the ~~unusually~~ depleted isotopic composition of precipitation and atmospheric water vapour (Fudeyasu et al., 2008; Jackisch et al., 2022; Munksgaard et al., 2015) due to a combination of strong cyclonic circulation, intense large-scale convection, heavy precipitation, and high wind speeds (Chen et al., 2021; Xu et al., 2019). ~~Here~~ W~~w~~e analysed the relationship between the isotopic composition ~~of atmospheric water vapour~~ and convective processes~~ during two cyclone events~~, using ~~outgoing longwave radiation (~~OLR~~)~~ and vertical velocity as a proxy for convection. Due to the frequent co-occurrence of intense convection and significant mid-tropospheric convergence of moist air, the vertical velocities can also serve as a proxy for convective activity (Lekshmy et al., 2014).

Fig. S~~5~~3 and Fig. S4~~6~~ depict the prevalence of strong convective processes associated with both cyclones throughout their ~~entire~~ lifespans. During the initial days of cyclone formation, OLR exceeded 260 Wm^{-2} in the area of the sampling site ~~(Figs. S5 and S6)~~ and ~~had rather~~ decreased rapidly to below 200 Wm^{-2} in the final stages of both cyclones when ~~they were~~ approaching the~~ sampling~~ site. Although the amount of precipitation associated with Tauktae (9.2 mm) was much lower than~~ with~~ Yaas (59.6 mm), $\delta^{18}O_v$ depleted by up to 12 ‰ during both cyclones~~ events~~. ~~Importantly, during both cyclones events, ~~T~~t~~he progressive rainout was evident along the entire cyclone track, and the spatial distribution of precipitation was highly correlated with the convective process, ~~(~~as indicated by low OLR.~~)~~ (Figs. S5~~7~~ and S6~~8~~), suggesting ~~that~~ rainfall occurred from the deep convective cloud rather than~~ from~~ local evaporation. This ~~interpretation ~~was confirmed by ~~comparing the regional ~~precipitation variations.~~to *in situ* measurements. According to Fig. S7 and Fig. S8, the~~The ~~measurement ~~site received its first rainfall on 19 May during cyclone Tauktae and on 25 May during cyclone Yaas, as shown in Figure S5 and Figure S6. ~~which we can confirm with our observation data.~~ *In situ* observations confirm~~show~~ that during the days leading up to cyclone Tauktae, the sampling site received a total of 12.2 mm~~m (from 7 May to 14 May)~~ of precipitation with maximum rainfall of 9.2 mm/h recorded on 11 May at 13:00 h LT, ~~which is~~ equal to the total accumulated rainfall during the entire cyclone Tauktae. Although the pre and~~ Tauktae and~~ during-Tauktae rainfall amounts are similar, pre-cyclone $\delta^{18}O_v$ and δD_v were significantly more enriched (averages:$\delta^{18}O_v$ = -10.04~~1.83~~ ‰ and δD_v = -69.51~~80.30~~ ‰) than ~~during~~ during Tauktae (averages: $\delta^{18}O_v$ = -14.73 ‰ and δD_v = -106.76 ‰) ~~the cyclone event (averages: $\delta^{18}O_v$ = -13.59 ‰ and δD_v = -149.49 ‰)~~. We compared the values of $\delta^{18}O_v$, δD_v, and d-excess$_v$ during both events and also examined them in comparison with the isotopic composition at the beginning of the summer monsoon (June 2021). This initial period of intense and continuous rainfall at our sampling site (Fig. S7) is regulated by the monsoon system originating in the BoB. Consequently, our focus centered on the isotopic distinctions between water vapour on typical rainy days and that associated with cyclone Yaas.

Following the initiation of the summer monsoon, both $\delta^{18}O_v$ and δD_v exhibited a progressive depletion, coinciding with a decline in air temperature, an increase in relative humidity (RH), and amplified rainfall amounts (Fig. S7). Despite the daily accumulated rainfall and RH being significantly higher during the normal monsoon period, both $\delta^{18}O_v$ and δD_v were markedly lower during cyclone Yaas (on average by over 2.5‰ and 26‰ for $\delta^{18}O_v$ and δD_v respectively) compared to typical rainy days. A progressive reduction in d-excess$_v$ was also evident as the summer monsoon unfolded; a trend typically observed in precipitation d-excess (e.g., Hussain et al., 2015; Acharya et al., 2020; Adhikari et al., 2020) and water vapour d-excess (Tian et al., 2020; Yao et al., 2018; He and Richards, 2016; Wei et al., 2016) in Asian monsoon regions, in contrast to our observations during cyclone Yaas.

Given that d-excess has long served as a diagnostic tool for understanding moisture source conditions (Tian et al., 2001; Liu et al., 2008), the distinct behaviour of d-excess$_v$ between cyclone Yaas and the normal monsoon phase suggests that cyclone-related information may be discerned through the isotopic composition recorded at our site. This confirms our previously stated hypothesis that ~~the~~ rainfall associated with cyclones causes significantly lower isotope values in vapour due to intense convective systems (Gedzelman et al., 2003; Kurita, 2013), ~~which is~~ absent in local~~ized~~ rain events and ~~on~~ days without precipitation (Lekshmy et al., 2022).

Formatted: Font color: Auto

The influence of convective processes on water vapor isotopic variations at Kathmandu ~~Our hypothesis that isotopic variations during cyclone events at Kathmandu are mainly driven by convective processes~~ is further supported by the Hovmöller diagram of OLR averaged over 80-90° E ~~(Figure 6)~~, which clearly shows that $\delta^{18}O_v$ depletion coincides with the presence of clouds (Figure 6 Time series of daily averaged d-excess$_v$ (top panel), $\delta^{18}O_v$ (middle panel), and Hovmöller diagram of OLR (W/m^2) averaged over 80° E-90° E (bottom panel) The solid parallel lines in the bottom panel depict the latitude range of sampling site.

7a and c). In contrast, d-excess$_v$ showed ~~rather~~ dissimilar variations between both cyclones~~ events~~. Before ~~the arrival of~~ cyclone Tauktae, the daily averaged d-excess$_v$ was above the global average of 10 ‰ (Fig. 7a~~6, horizontal orange line~~). Once Tauktae approached our ~~was approaching the~~ sampling site, d-excess$_v$ decreased from around 12 ‰ to 10 ‰ and continued to oscillate about 10 ‰ until Tauktae had dissipated. As cyclone Yaas approached the measurement site with intense rainfall (Fig. 3~~2~~), d-excess$_v$ ~~($\delta^{18}O_v$)~~ gradually increased ~~(decreased)~~ while RH increased and air temperature decreased (Fig. 3~~2~~). ~~More s~~Specifically, d-excess$_v$ on 24 May was recorded as 12.82 ‰ when surface air temperature and surface RH was about 24 °C and 70 % respectively. On 27 May, we not~~ed~~iced ~~about~~ a 3 ‰ rise in d-excess$_v$ when the surface temperature was reduced by 4 °C and the surface RH was increased by 19 %. The combination of increasing d-excess and decreasing $\delta^{18}O_v$ has also been observed during the active convective phase of Madden-Julian oscillations (MJO) in the tropical atmosphere which highlights the role of vapour recycling due to the subsidence of air masses from stratiform clouds (Kurita et al., 2011). In addition, a large increase in d-excess$_v$ was also recorded in atmospheric vapour during cyclone Ita in 2014 and was attributed to downward moisture transport above the boundary layer (Munksgaard et al., 2015). In our case, Wwe did not find any statistically significant correlation during cyclone Yaas between d-excess$_v$ and RH/Temperature, although RH is generally considered an important parameter for interpreting d-excess values in atmospheric vapour and precipitation (Pfahl and Sodemann, 2014; Steen-Larsen et al., 2014). The observed co-occurrence of higher d-excess$_v$, lower temperatures, and high relative humidity (Fig. 32) points to kinetic fractionation processes either at a larger scale or in association with downdrafts (Conroy et al., 2016). Rain re-evaporation under the condition of high saturation deficit is one of the causes of low $\delta^{18}O_v$ and high d-excess$_v$. This is due to the addition of re-evaporated vapour during precipitation events, which results in depleted cloud vapour and high d-excess$_v$ (Conroy et al., 2016; Lekshmy et al., 2014).This relationship also highlights the role played by the convective process with regard to the isotopic composition of atmospheric water vapour. Low $\delta^{18}O_v$ in combination with high d-excess$_v$ are known to be associated with rain re-evaporation under conditions of high saturation deficit because the addition of re-evaporated vapour to the atmosphere during precipitation events produces depleted cloud vapour and high d-excess (Conroy et al., 2016; Lekshmy et al., 2014). On normal days (without cyclones), high d-excess$_v$ values were generally accompanied by low RH (Figure Figure 78) and vice versa. However, high relative humidities of the surface air together with near saturation conditions vertically (Figure Figure 89b, middle panel) during cyclone Yaas, rule out any effect of re-evaporation on increased (decreased) d-excess$_v$ ($\delta^{18}O_v$ and δD_v) values. Such high d-excess$_v$ values mayHence, we surmise that the higher d-excess$_v$ values during cyclone Yaas might be associated with downdrafts during convective rain events, which can transporting isotopically depleted vapour with higher d-excess$_v$ values from the boundary layer to the surface (Kurita, 2013; Midhun et al., 2013).

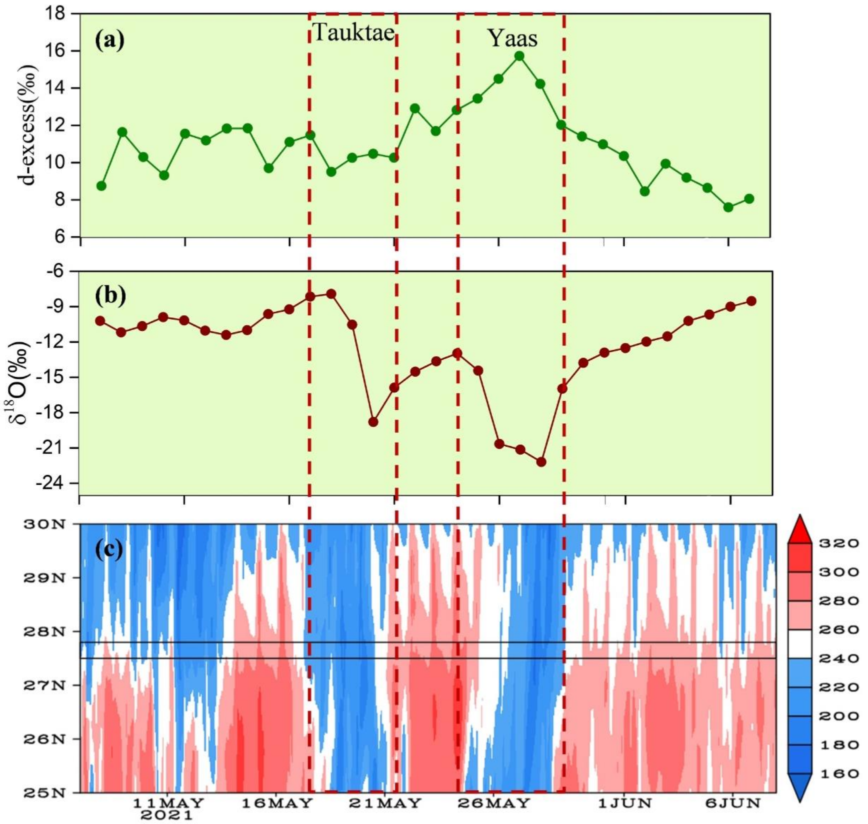

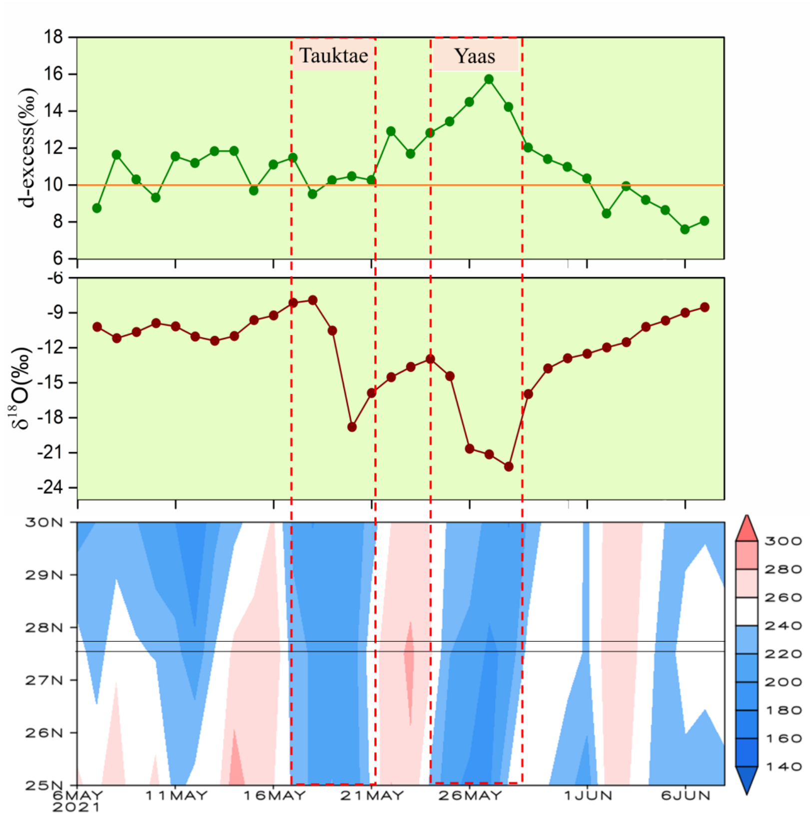

Figure 6 Time series of daily averaged d-excess$_v$ (top panel), $\delta^{18}O_v$ (middle panel), and Hovmöller diagram of OLR (W/m^2) averaged over 80° E-90° E (bottom panel) The solid parallel lines in the bottom panel depict the latitude range of sampling site.

~~**Figure 6 Time series of daily averaged d-excess$_v$ (top panel), $\delta^{18}O_v$ (middle panel), and Hovmöller diagram of NOAA interpolated OLR (W/m^2) averaged over 80° E-90° E (bottom panel) The orange horizontal line in the top panel represents the global average d-excess value (i.e. 10 ‰) and solid parallel lines in bottom panel depict the latitude range of sampling site.**~~

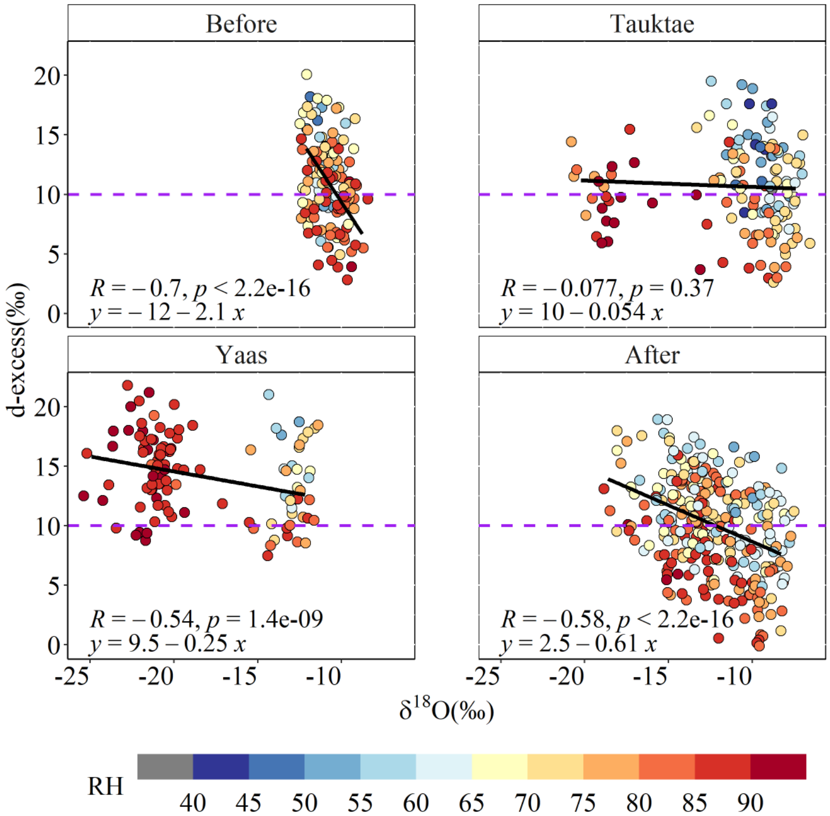

Figure ~~7~~ 8 Scatter plots of d-excess$_v$ vs. $\delta^{18}O_v$ before, during, and after the cyclone events. The colour represents RH (in %) and the horizontal dashed purple lines represent the global average d-excess value (10 ‰).

To ~~further elucidate~~clarify the impact of convection on the isotopic composition~~ of atmospheric water vapour~~, we analys~~z~~ed the vertical distribution of vertical velocity, relative humidity, and air temperature averaged over a box between 25° N-28° N and 83° E-87° E with~~hich has~~ our measurement site near its center~~re~~ (Fig. 9~~8~~). Our results show that strong shifts in $\delta^{18}O_v$, δD_v, and d-excess$_v$ during the cyclone events were strongly associated with vertical air motions (Figure 8Fig. 9c). We observed a general downward movement of air before the rain started with Tauktaebefore the commencement of rainfall by Tauktae (i.e., from 7 May to around 18 May). The high depletion of $\delta^{18}O_v$ and δD_v during the final stages of Tauktae (Figure 2Fig. 3) was accompanied by strong upward air movement extending from 800 hPa to about 200 hPa (Figure 8Fig. 9c). This upward motion was even stronger during cyclone Yaas and already became evident near the measurement site once Yaas made landfall at the BoB coast on 26 May. Interestingly, variations in RH at different pressure levels strongly coincided with changes in vertical velocity while the lower troposphere remained near saturation (RH= ~100 %) during the late stages of both cyclones (Fig. 9b). While the vertical air temperature showed the expected progressive decline with altitude (Fig. 9a), there were no significant temporal variations in temperature during the entire period, despite the high variation in RH. This implies that the high RH in the lower troposphere during both cyclone events was independent of temperature and hence the result of deep convection and the widespread development of clouds. The strong convective updraft added additional moisture from the warm ocean below, before passing over our measurement site (Lekshmy et al., 2014). Convective updrafts cause moisture to condense quickly and this high-efficiency condensation of heavy rain can result in more depleted $\delta^{18}O_v$ and δD_v (Lawrence and Gedzelman, 1996). In addition, we found a strong positive correlation between- $\delta^{18}O_v$ and average vertical velocity (r=0.57) during Yaas at pressure levels between 300 hPa and 600 hPa (Fig. S8a) in the area surrounding our study site. (cf., Lekhsmy et al., 2014); During Tauktae, tThis correlation was weaker but still significant (r=0.30) (Fig. S9) during Tauktae. The distinctive relationship between $\delta^{18}O_v$ and vertical velocity implies that convective processes play a more significant role during Yaas than Tauktae. This result was further supported by the spatial distribution of correlation coefficient between $\delta^{18}O_v$ and vertical velocity

(Fig. S8b, c). During cyclone Tauktae, a significant negative correlation was observed between $\delta^{18}O_v$ and vertical velocity around the sampling site, while positive correlation areas were identified in western Nepal, certain parts of central India, and the coastal region of the Bay of Bengal (BoB) (Fig. S8b). A comparison with back trajectories unveiled positive correlation only in specific sections along the moisture transport path, suggesting that convective processes may not be the primary driver of isotopic depletion during cyclone Tauktae. Conversely, a positive correlation was evident in the coastal BoB, extending north toward the sampling site during cyclone Yaas (Fig. S8c). The positive correlation areas were considerably larger compared to Tauktae, and these areas closely aligned with the moisture transport path. Hence, higher depletion in $\delta^{18}O_v$ and δD_v during Yaas, relative to Tauktae, may be attributed to the stronger convection associated with BoB vapour compared to the AS vapourThis result suggests that the higher depletion in $\delta^{18}O_v$ and δD_v during cyclone Yaas relative to Tauktae may be due to the stronger convection associated with the BoB vapour compared to the AS vapour. The BoB is a convectively active region, and previous studies reported greater depletions in $\delta^{18}O_v$ and δD_v in precipitations with moisture from the BoB compared to the AS, irrespective of the season (Breitenbach et al., 2010; Lekshmy et al., 2015; Midhun et al., 2018). Another reason why we observed different levels of isotope depletion between both cyclones may be related to differences in their closest proximity to the sampling site. While Yaas came as close as 400 km to our study site, Tauktae was still 1100 km away when it dissipated (Fig. S910). The closer proximity of Yaas may explain the stronger rainfall during that event which enhanced the isotopic fractionation which in turn leadingd to stronger isotopic depletion (Jackisch et al., 2022). Similar results during the cyclone events have already been documented for precipitation stable isotopes (e.g., Fudeyasu et al., 2008; Jackisch et al., 2022; Munksgaard et al., 2015; Xu et al.,

2019) and water vapour stable isotopes (e.g., Munksgaard et al., 2015; Rahul et al., 2016; Saranya et al., 2018). Even after both cyclones had dissipated, progressive rainfall continued at our sampling site due to the presence of residual moisture from the cyclones. Once these residual effects had diminished and rainfall intensity weakened, did both $\delta^{18}O_v$ and δD_v started to increase again (Fig. 32), likely due to evaporative effects (Munksgaard et al., 2015; Xu et al., 2019; Jackisch et al., 2022).

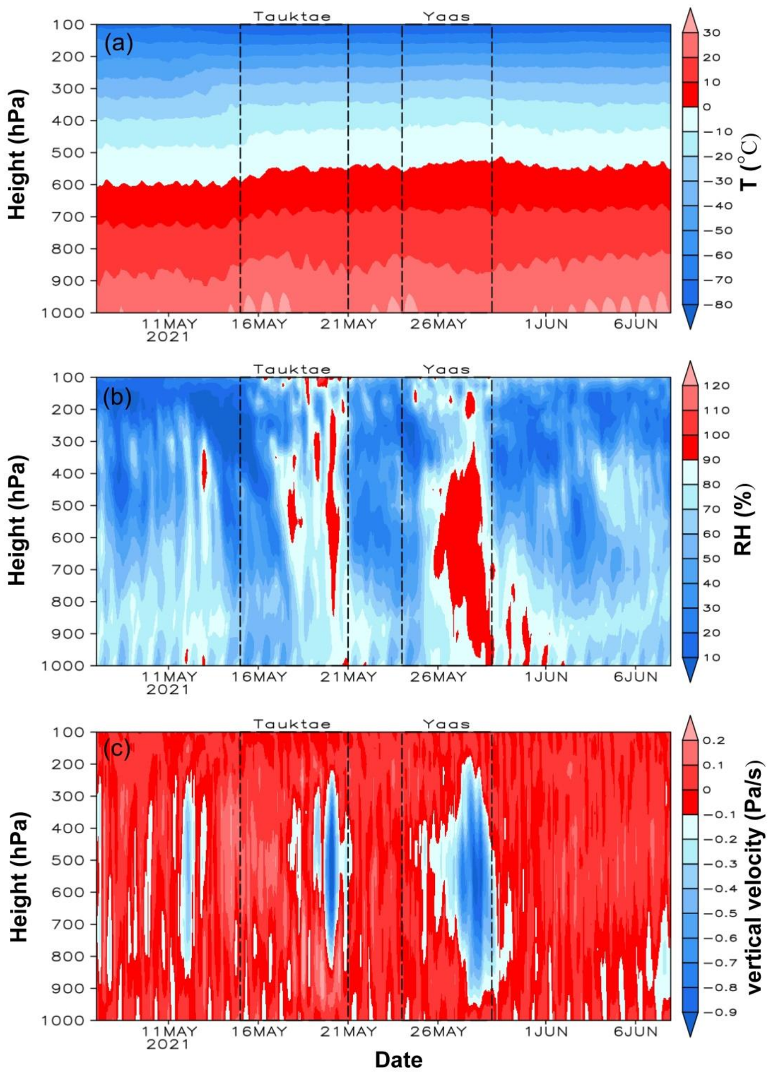

Figure 8 9 Time series of the vertical distribution of air temperature (a), RH (b), and vertical velocity (c) averaged over 25° N-28° N and 83° E-87° E with Kathmandu approximately at the centre. Negative (positive) vertical velocities indicate ascending (descending) winds.Time series of the vertical distribution of air temperature (top), RH

(middle), and vertical velocity (bottom) averaged over 25° N-28° N and 83° E-87° E with Kathmandu approximately at the centre. Negative (positive) vertical velocities indicate ascending (descending) winds.

Examining a plot of δD_v vs specific humidity, combined with the Rayleigh distillation and mixing curves, we can assess the mixing conditions during the study period (Figure 9). Before the development of cyclone Tauktae and during its early stages, the data points lie well above the mixing curve, suggesting a significant contribution of vapour from local evapotranspiration. In contrast, during the later stages of Tauktae, δD_v was significantly depleted to levels well below the Rayleigh curve. Similarly, during the early stage of cyclone Yaas, there are only a few data points between the mixing and Rayleigh curves with the majority well below the Rayleigh curve, particularly during the late stage of Yaas. These results indicate the influences of mixing processes and re-evaporation below clouds as described previously (Galewsky and Samuels-Crow, 2015). After Yaas had dissipated, δD_v gradually increased again with about half of the data points clustered between the mixing and Rayleigh curves and the remaining data points well above the mixing curve, indicating a strong influence of mixing processes and locally evaporated vapour, which is also evidenced by the moisture backward trajectories (Figure 5 lower right panel).

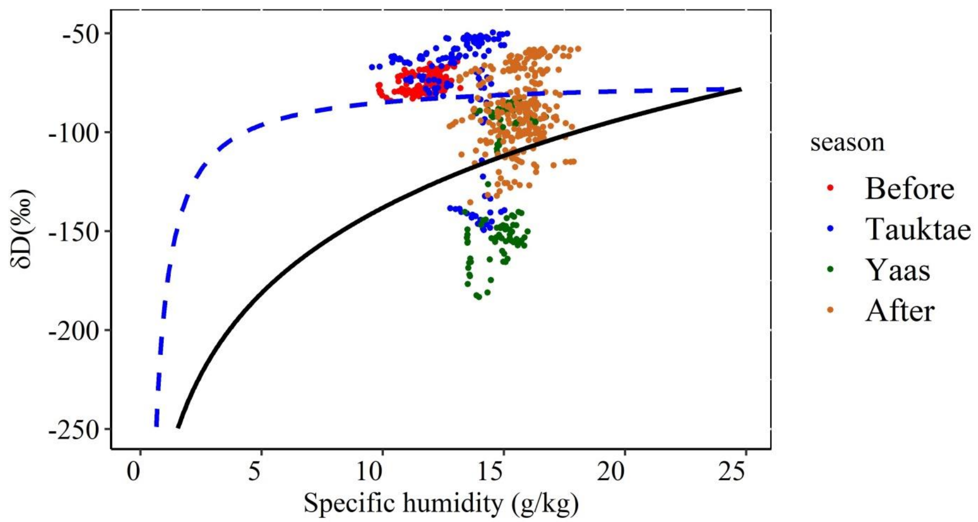

Figure 9 Scatter plot of hourly averaged δD_v vs. specific humidity (q). The solid black curve represents the Rayleigh distillation curve calculated for the initial condition of δD_v = - 78.20 ‰, BoB-averaged δD_v (Lekshmy et al., 2022), SST of 30° C, and RH of 90 %. The dashed blue curve represents the mixing line, calculated based on dry continental air (q= 0.5 g/kg and δD_v =-300 ‰ (Wang et al., 2021)) and the wet source, which corresponds to the initial conditions used to calculate the theoretical Rayleigh curve.

3.4 Relationships between local weather parameters and vapour $\delta^{18}O$, δD, and d-excess

Besides regional influences, we also analyzed whether changes in local meteorological conditions impact the variations in the isotopic composition of atmospheric water vapour. Before the cyclone events, both $\delta^{18}O_v$ and δD_v showed significant negative correlations with local air temperature and wind speed and significant positive correlations with relative humidity (Table 2). This correlation between $\delta^{18}O_v$/δD_v and relative humidity became negative during the two cyclone events, with a significant temperature effect also present. We hypothesize that the progressive rainout during the cyclone events followed a temperature decrease (Figure 2), which would result in this $\delta^{18}O_v/\delta D_v$ correlation with temperature (Delattre et al., 2015). However, the strength of the correlations between $\delta^{18}O_v/\delta D_v$ and local meteorological parameters varied significantly throughout the lifetimes of both cyclones. For instance, the effects of temperature and relative humidity on $\delta^{18}O_v$ were stronger ($r=0.68$ for temperature and $r=-0.74$ for RH) during Yaas compared to Tauktae ($r=0.34$ for temperature and $r=-0.49$ for relative humidity). The weaker relationship during Tauktae is likely due to the significantly lower rainfall amounts relative to Yaas. The cooling of surface air during rainfall and the associated isotopic equilibrium of vapour with raindrops cause a positive correlation between $\delta^{18}O_v/\delta D_v$ and temperature (Midhun et al., 2013). This process was more favourable during Yaas with its stronger and more continuous rainfall (Fig. 2). During Tauktae, we did not observe any effect of precipitation amount on the isotopic composition of atmospheric water vapour, while during Yaas there was a strong negative correlation ($r=-0.56$) between them. Recent studies have suggested that the impact of rainfall amount is not a purely local phenomenon (Galewsky et al., 2016) but modulated by convective and large-scale properties such as downdraft moisture recycling (Risi et al., 2008), large-scale organized convection and associated stratiform rain (Kurita, 2013), and regional circulation and shifting moisture source regions (Lawrence et al., 2004). During cyclone Yaas, our measurements showed the presence of an intense convective system over our study site which indicates that the observed rainfall amount effect may have been controlled by moisture convergence (Chakraborty et al., 2016). Subsequent rainfall from the convective system over a region with depleted isotope values resulted in a negative association between precipitation amount and $\delta^{18}O_v/\delta D_v$ (Kurita, 2013). Furthermore, the negative correlation between $\delta^{18}O_v/\delta D_v$

and RH together with the fact that $\delta^{18}O_v$/δD_v was depleted during both cyclone events highlight the influence of humid moisture sources on the isotopic composition of atmospheric water vapour (Yu et al., 2008), which was also confirmed by our moisture backward trajectory analysis (Fig. 5). A strong negative correlation between δD_v and RH was also observed in mid-tropospheric water vapour over the western Pacific associated with intense convective activity (Noone, 2012). It is noteworthy that the relationship between $\delta^{18}O_v$/δD_v and temperature before and after the cyclone events degraded significantly, which might be due to the admixture of vapour originating from plant transpiration during that period (Delattre et al., 2015).

As discussed above, $\delta^{18}O_v$ and δD_v were strongly associated with air temperature and RH during cyclone Yaas but less so during cyclone Tauktae. In contrast, d-excess$_v$ was positively (negatively) correlated with local air temperature (local RH) before, during Tauktae, and after both cyclone events, whilst no significant correlations were seen during cyclone Yaas (Table 2). This indicates that local moisture recycling may have played a crucial role at our sampling site, while the absence of any correlation of d-excess$_v$ with RH during Yaas implies that RH might not be a reliable predictor of kinetic fractionation during evaporation at our site. In addition, while about 75% of RH measurements during Yaas yielded high values (i.e., RH >80%), this fraction was only 25% during Tauktae. Previous studies (e.g., Midhun et al., 2013; Uemura et al., 2008) highlighted that the relation between d-excess$_v$ and RH weakens above RH=80%, which may explain the weaker relation of d-excess$_v$ and RH during Yaas.

Table 2 Linear correlations between the isotopic composition of atmospheric water vapor ($\delta^{18}O_v$, δD_v, and d-excess$_v$) and air temperature (T), relative humidity (RH), precipitation amount (P), wind speed (WS), and dew point temperature (T_d) before, during, and after the cyclone events. *,**, and * indicate correlation significance levels of 0.001, 0.01, and 0.05 respectively.**

	T	RH	P	WS	T_d
Before					
$\delta^{18}O_v$	-0.34***	0.45***	-0.41	-0.45***	0.16
δD_v	-0.1	0.28***	-0.37	-0.28***	0.41***
d-excess$_v$	0.68***	-0.61***	0.35	0.59***	0.40***
Cyclone Tauktae					
$\delta^{18}O_v$	0.34***	-0.49***	0.11	0.20*	-0.22**
δD_v	0.41***	-0.55***	0.10	0.26**	-0.20**
d-excess$_v$	0.79***	-0.67***	-0.22	0.75***	0.19*
Cyclone Yaas					
$\delta^{18}O_v$	0.68***	-0.74***	-0.56***	0.05	0.28**
δD_v	0.70***	-0.76***	-0.56***	0.06	0.30**
d-excess$_v$	-0.003	0.1	0.19	0.27**	0.19*
After					
$\delta^{18}O_v$	0.13*	-0.13*	-	0.14*	0.10
δD_v	0.22***	-0.22***	-	0.21***	0.18**
d-excess$_v$	0.56***	-0.54***	-	0.47***	0.47***

4.3 Influence of rainfall

The back trajectories reveal the impact of separate air masses during cyclones Tauktae and Yaas, specifically between the AS and BoB. We studied the meteorological conditions along the 5-day moisture back trajectories, focusing on the upstream rainout on observed isotopic depletion. During cyclone Tauktae, both $\delta^{18}O_v$ and δD_v display a strong negative correlation (r= -0.80 and r= -0.79 for $\delta^{18}O_v$ and δD_v, respectively, Fig. 10) with total precipitation along the moisture trajectories (i.e., upstream rainout). Moreover, a negative correlation emerges between $\delta^{18}O_v$/δD_v and average relative humidity (RH) along the trajectories (r= -0.69 for $\delta^{18}O_v$ and -0.68

Formatted: List Paragraph, Left, Line spacing: single, Outline numbered + Level: 2 + Numbering Style: 1, 2, 3, … + Start at: 1 + Alignment: Left + Aligned at: 0" + Indent at: 0.4" for δD_v), suggesting increased upstream rainout corresponds to lower isotope ratios during cyclone Tauktae.

In addition, modelled back trajectories indicate that air masses during cyclone Tauktae had a longer transport time when continuous rainout could have enhanced the isotopic depletion of the residual vapour (Fig. 5b). The upstream rainfall control could also account for the delayed return of $\delta^{18}O_v$ and δD_v to more positive values following dissipation.

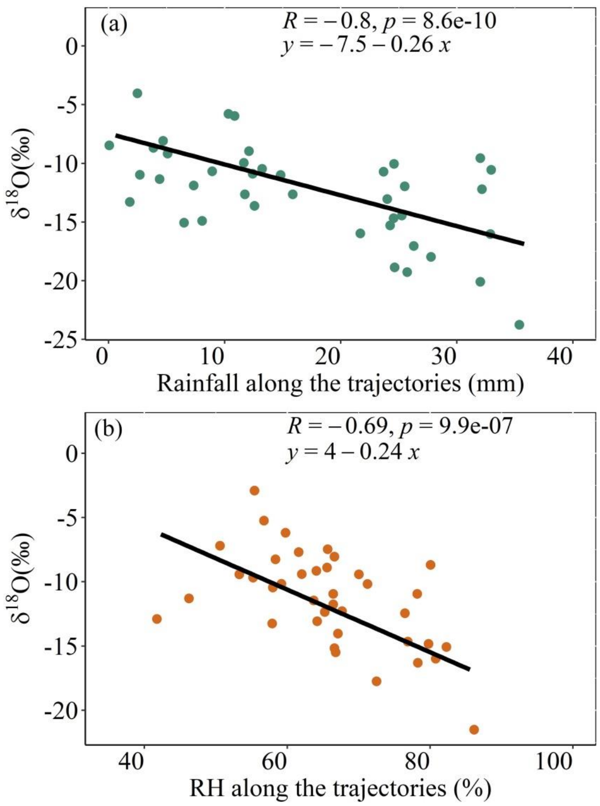

Figure 7 (a) Scatter plots of $\delta^{18}O_v$ vs upstream rainout and (b) average relative humidity (RH) along the moisture trajectories during the cyclone Tauktae.

Similar observations have been documented in other regions; for example, the Chinese Typhoons Haitang, Megi, and Soudelor (Xu et al., 2019), the Central American Hurricanes Irma and Otto (Sánchez-Murillo et al., 2019), and Central Texas Hurricane Harvey (Sun et al., 2022) all demonstrate significant negative correlations between upstream rainout and precipitation $\delta^{18}O$. This suggests that upstream rainout could serve as a widely applicable control on the spatiotemporal variability in tropical cyclones (Sun et al., 2022).

In contrast to cyclone Tauktae, neither the total rainfall nor the relative humidity (RH) along the trajectories appears to exert influence on isotopic variation during cyclone Yaas. Instead, a negative correlation was observed between $\delta^{18}O_v/\delta D_v$ and local rainfall amount, air temperature, and RH (Table 2). This suggests that the observed isotopic depletion during cyclone Yaas cannot be adequately explained by upstream rainout processes. We assume that sudden changes in local meteorological conditions are a consequence of synoptic processes during the cyclones. The progressive rainout during the cyclone events followed a temperature decrease () which would result in the $\delta^{18}O_v/\delta D_v$ correlation with temperature (Delattre et al., 2015). The cooling of surface air during rainfall, coupled with the isotopic equilibrium of vapour with raindrops, establishes a positive correlation between $\delta^{18}O_v/\delta D_v$ and temperature (Midhun et al., 2013). These conditions were favourable during cyclone Yaas because the sampling site experienced consistent rainfall, along with a noticeable increase in relative humidity and a decrease in temperature. This might be one of the reasons for the weaker correlation of $\delta^{18}O_v/\delta D_v$ with local meteorological variables during Tauktae.

Studies have speculated that the impact of precipitation amount is not confined to a strictly local context (Galewsky et al., 2016), but is subject to modulation by convective and large-scale atmospheric properties including downdraft moisture recycling (Risi et al., 2008), large-scale organized convection and associated stratiform rain (Kurita, 2013), as well as regional circulation and shifting moisture sources (Lawrence et al., 2004). Our measurements during cyclone Yaas revealed the presence of an intense convective system over our study site, indicating that the observed effect of rainfall amount may have been governed by moisture convergence (Chakraborty et al., 2016). The subsequent rainfall originating from the convective system, occurring over a region characterized by depleted isotope values, resulted in a negative association between precipitation amount and $\delta^{18}O_v$/δD_v (Kurita, 2013). The ^{18}O-depleted water vapour reaching the sub-cloud layer, accompanied by the intense convective downdrafts, subsequently ascended back to the cloud level with the updrafts, in a feedback mechanism proposed by Lekshmy et al., (2014).

Given that CTT and CTP are reliable indicators of both moisture convergence and convective strength in prior studies (Cai et al., 2018; Cai and Tian, 2016), we investigate the linear correlation between CTT/CTP (averaged over the 27°N-28°N latitude and 85°E-86°E longitude range, with our site located at the center) and $\delta^{18}O_v$ (Fig. 11). The results demonstrate a weak positive correlation between CTT/CTP and $\delta^{18}O_v$ during cyclone Tauktae, and a robust positive correlation during cyclone Yaas. These correlations exhibit greater strength compared to the correlation observed with local rainfall. Previous research has highlighted positive correlations between $\delta^{18}O$ and CTT/CTP in the East Asian Monsoon suggesting that intense convection and moisture convergence lead to an increase in cloud-top height and a decrease in CTT, causing a reduction in $\delta^{18}O$ (Cai and Tian, 2016). The decrease in $\delta^{18}O_v$ during cyclone Yaas coupled with a decrease in CTT and CTP (i.e. increase in cloud-top height), shows the influence of intensified convective activities and moisture convergence, while the isotopic depletion during cyclone Tauktae is attributed to upstream rainout processes. Furthermore, a negative correlation is evident between d-excess$_v$ and CTT/CTP, with r = -0.52 and r = -0.60 during cyclone Yaas. Conversely, a weak positive correlation is observed during cyclone Tauktae, with r = 0.32 for both CTT and CTP. This relationship implies that lower CTT and CTP during intense convection relate to increased d-excess$_v$ values during the final stage of cyclone Yaas.

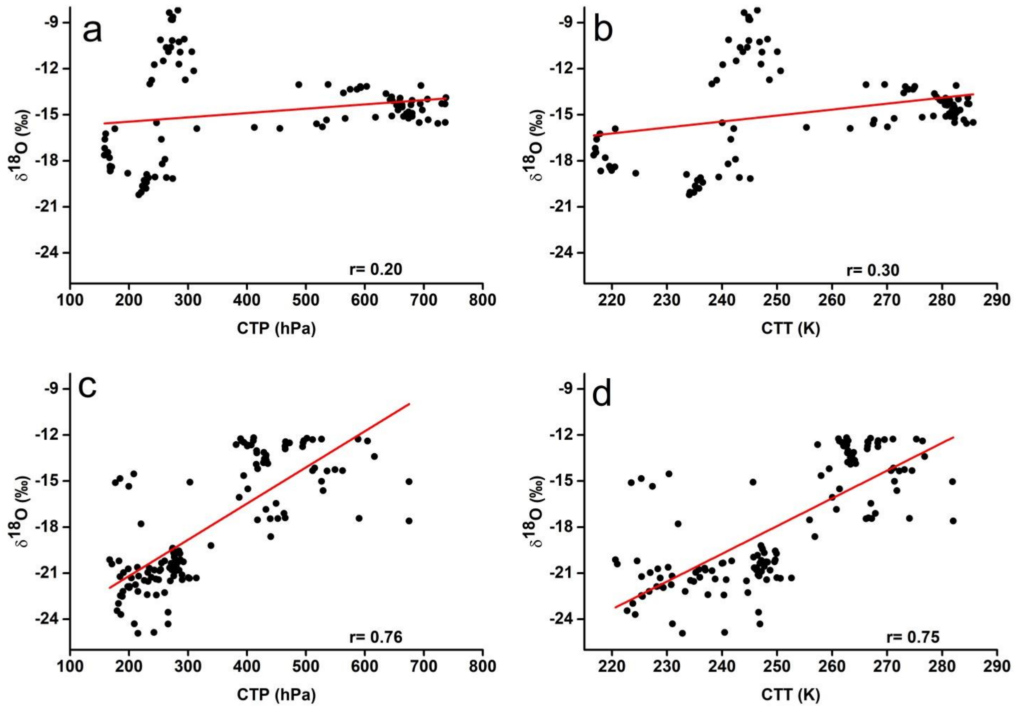

Figure 8 Relationship between hourly $\delta^{18}O_v$ and (a) CTT during Tauktae, (b) CTP during Tauktae, (c) CTT during Yaas, and (d) CTP during Yaas.

~~4~~5 Conclusion

This study presented the results of continuous measurements of the isotopic composition of atmospheric water vapour over Kathmandu between 7 May and 7 June 2021 covering two cyclone events;~~,~~ ~~namely~~ cyclone Tauktae formed over the Arabian Sea, and cyclone Yaas formed over the Bay of Bengal. $\delta^{18}O_v$ (δD_v) during Tauktae varied from -8.20‰ (-56.06‰) to -20.21‰ (-149.49‰) with an average of -14.73‰ (-106.76‰) and during Yaas $\delta^{18}O_v$ (δD_v) ranges from -12.17‰ (-83.85‰) to -24.92‰ (-183.34‰) with an average of -17.87‰ (-129.18‰). Similarly, d-excess$_v$ during Tauktae varied from 7.97 ‰ to 14.24 ‰ with an average of 11.06 ‰ while during Yaas it varied from 8.71 ‰ to 18.29 ‰ with an average of 13.77 ‰. Both cyclones ~~events~~ led to significant depletion of ~~–~~$\delta^{18}O_v$ and δD_v, with $\delta^{18}O_v$ decreasing by over 12 ‰ ~~between May 14 and May 20 (during Tauktae) as well as between May 24 and May 29 (during Yaas)~~. We~~ could~~ attribute these~~ose~~ rapid depletions to changes in moisture sources (local vs. marine) ~~that were~~ inferred from backward moisture trajectories. ~~Similar slopes and intercepts of meteoric vapour line with GMWL during both cyclone events indicate the occurrence of surface recharge following convective conditions.~~ The lower intercepts of the local meteoric vapour line before and after the ~~cyclone~~ events highlight the influence of non-equilibrium processes such as evaporation on the isotopic composition ~~of atmospheric water vapour~~.

~~Despite significant diurnal fluctuations in temperature and specific humidity during both cyclone events, $\delta^{18}O_v$ and δD_v exhibit weak diurnal signals which rule out any impact of day-night variations in local weather parameters. Instead, these discrepancies might reflect different cyclone sources and convection processes they underwent along their northward trajectories.~~ The spatial distribution of OLR, vertical velocity, and regional precipitation during both cyclonice events ~~together with the observed correlation between vertical velocity and $\delta^{18}O_v$~~ indicated significantshowed high moisture convergence and heavy intense convection at and around the measurement site. which caused unusuallyThis resulted in depleted $\delta^{18}O_v$ and δD_v, with cyclone Yaas exhibiting stronger moisture convergence and convection, leading to lower $\delta^{18}O_v$ values compared to cyclone Tauktae. during that period. Moisture convergence and convection were stronger during cyclone Yaas which resulted in higher (lower) d-excess$_v$ ($\delta^{18}O_v$) values during Yaas, compared to Tauktae, possibly due This difference may be attributed to strongrobust downdrafts during the cycloneYaas-related convective rain events, which canpotentially transporting vapour with higher (lower) d-excess$_v$ and lower ($\delta^{18}O_v$) values toward the surface. The observed isotopic depletion during cyclone Tauktae can be explained by upstream rainout processes, unlike during Yaas. During the cyclone events, and in contrast to immediately before and after these events, there was a strong linear association between the isotopic compositions of atmospheric water vapour and local meteorological parameters, which led us to conclude that the progressive rainout during the cyclone events followed a temperature decrease and RH increase, which would, in turn, produce a $\delta^{18}O_v$/δD_v correlation with temperature and RH. This type of association may visible in the cyclones' moisture characteristics as each cyclone transported high RH from a remote ocean inland, which suggested that their specific water vapour stable isotopic signatures could still be observed as far north as Kathmandu.

Overall, our results showed that tropical cyclones that originatinged in the BoB and the AS during the pre-monsoon season transported large amounts of isotopically depleted vapour and produced moderate to heavy rainfall over a sizeable region in Nepal. The isotopic composition of atmospheric water vapour and precipitation during the dry season should therefore Hence the isotopic composition of atmospheric water vapour and precipitation during the dry season should be be interpreted with caution and the effects of cyclones should not be underestimated. AdditionallyIn addition, our results further underline the need for simultaneous measurements of the isotopic composition of both atmospheric water vapour and precipitation to better understand post-condensation exchanges between falling raindrops and boundary layer vapour over Kathmandu.

Data Availability

The data used in this study will be available in the Zenodo repository.

Data will be available upon request from the corresponding author.

Competing interests

The contact author has declared that none of the authors has any competing interests.

Acknowledgements

This work was funded by 'The Second Tibetan Plateau Scientific Expedition and Research (STEP) project' (Grant No. 2019QZKK0208) and the National Natural Science Foundation of China (Grants 41922002 and 41988101-03). We thank Yulong Yang for his assistance with instrument set-up and initial running.

Author contributions

Niranjan Adhikari: Data curation, Formal analysis, Writing - Original draft preparation. **Jing Gao**: Data curation, Conceptualization, Methodology, Supervision, Writing - Review and Editing, Funding acquisition. **Aibin Zhao**: measuring assistance, Writing – Editing. **Tianli Xu**, **Manli Chen,** and **Xiaowei Niu**: measuring assistance. **Tandong Yao**: Supervision, Funding acquisition.

References

Acharya, S., Yang, X., Yao, T., Shrestha, D.: Stable isotopes of precipitation in Nepal Himalaya highlight the topographic influence on moisture transport, Quat. Int., 565, 22–30, https://doi.org/10.1016/j.quaint.2020.09.052, 2020.

Adhikari, N., Gao, J., Yao, T., Yang, Y., Dai, D.: The main controls of the precipitation stable isotopes at Kathmandu, Nepal, Tellus, Ser. B Chem. Phys. Meteorol., 72, 1–17. https://doi.org/10.1080/16000889.2020.1721967, 2020

Bohlinger, P., Sorteberg, A., Sodemann, H.: Synoptic conditions and moisture sources actuating extreme precipitation in Nepal, J. Geophys. Res. Atmos., 122, 12–653, https://doi.org/10.1002/2017JD027543, 2017.

Boschi, R., Lucarini, V.: Water pathways for the Hindu-Kush-Himalaya and an analysis of three flood events, Atmosphere, 10, 489, https://doi.org/10.3390/atmos10090489, 2019.

Brand, W.A., Geilmann, H., Crosson, E.R., Rella, C.W.: Cavity ring-down spectroscopy versus high-temperature conversion isotope ratio mass spectrometry; a case study on delta (2) H and delta (18) O of pure water samples and alcohol/water mixtures, Rapid Commun. mass Spectrom, RCM 23, 1879–1884, https://doi.org/10.1002/rcm.4083, 2009.

Breitenbach, S.F.M., Adkins, J.F., Meyer, H., Marwan, N., Kumar, K.K., Haug, G.H.: Strong influence of water vapor source dynamics on stable isotopes in precipitation observed in Southern Meghalaya, NE India, Earth Planet. Sci. Lett., 292, 212–220, https://doi.org/10.1016/j.epsl.2010.01.038, 2010.

Chakraborty, S., Sinha, N., Chattopadhyay, R., Sengupta, S., Mohan, P.M., Datye, A., 2016. Atmospheric controls on the precipitation isotopes over the Andaman Islands, Bay of Bengal, Sci. Rep., 6, 1–11, https://doi.org/10.1038/srep19555, 2016.

Chan, K.T.F., Chan, J.C.L., Zhang, K., Wu, Y.: Uncertainties in tropical cyclone landfall decay, npj Clim. Atmos. Sci., 5, 93, https://doi.org/10.1038/s41612-022-00320-z, 2022.

Chen, F., Huang, C., Lao, Q., Zhang, S., Chen, C., Zhou, X., Lu, X., Zhu, Q.: Typhoon Control of Precipitation Dual Isotopes in Southern China and Its Palaeoenvironmental Implications, J. Geophys. Res. Atmos., 126, 1–15, https://doi.org/10.1029/2020JD034336, 2021.

Chhetri, T.B., Yao, T., Yu, W., Ding, L., Joswiak, D., Tian, L., Devkota, L.P., Qu, D.: Stable isotopic compositions of precipitation events from Kathmandu, southern slope of the Himalayas, Chinese Sci. Bull., 59, 4838–4846, https://doi.org/10.1007/s11434-014-0547-4, 2014.

Conroy, J.L., Noone, D., Cobb, K.M., Moerman, J.W., Konecky, B.L.: Paired stable isotopologues in precipitation and vapor: A case study of the amount effect within western tropical Pacific storms, J. Geophys. Res. Atmos., 121, 3290–3303, https://doi.org/10.1002/2015JD023844, 2016.

Dansgaard, W.: Stable isotopes in precipitation, Tellus 16, 436–468, https://doi.org/10.3402/tellusa.v16i4.8993, 1964

Delattre, H., Vallet-Coulomb, C., Sonzogni, C.: Deuterium excess in the atmospheric water vapour of a Mediterranean coastal wetland: Regional vs. local signatures, Atmos. Chem. Phys., 15, 10167–10181, https://doi.org/10.5194/acp-15-10167-2015, 2015

Draxler, R.R., Hess, G.D.: Description of the HYSPLIT4 modeling system, 1997.

Fudeyasu, H., Ichiyanagi, K., Sugimoto, A., Yoshimura, K., Ueta, A., Yamanaka, M.D., Ozawa, K.: Isotope ratios of precipitation and water vapor observed in Typhoon Shanshan, J. Geophys. Res. Atmos, https://doi.org/10.1029/2007JD009313, 113, 2008.

Galewsky, J., Samuels-Crow, K.: Summertime moisture transport to the southern South American Altiplano: Constraints from in situ measurements of water vapor isotopic composition, J. Clim., 28, 2635–2649, https://doi.org/10.1175/JCLI-D-14-00511.1, 2015.

Galewsky, J., Steen-larsen, H.C., Field, R.D., Risi, W.C., Schneider, M.: Stable isotopes in athmospheric water vapor and application to the hydrologic cycle., Rev. Geophys. submitted, 1–169, https://doi.org/10.1002/2015RG000512, 2016.

Gaona, M.F.R., Villarini, G., Zhang, W., Vecchi, G.A.: The added value of IMERG in characterizing rainfall in tropical cyclones, Atmos. Res., doi:10.1016/j.atmosres.2018.03.008, 209, 95–102, 2018.

Gedzelman, S., Lawrence, J., Gamache, J., Black, M., Hindman, E., Black, R., Dunion, J., Willoughby, H., Zhang, X.: Probing hurricanes with stable isotopes of rain and water vapor, Mon. Weather Rev, https://doi.org/10.1175/1520-0493(2003)131<1112:phwsio>2.0.co;2, 131, 1112–1127, 2003.

Han, X., Lang, Y., Wang, T., Liu, C.Q., Li, F., Wang, F., Guo, Q., Li, S., Liu, M., Wang, Y., Xu, A.: Temporal and spatial variations in stable isotopic compositions of precipitation during the typhoon Lekima (2019), China. Sci. Total Environ., 762, https://doi.org/10.1016/j.scitotenv.2020.143143, 2021

Hassenruck-Gudipati, H.J., Andermann, C., Dee, S., Brunello, C.F., Baidya, K.P., Sachse, D., Meyer, H., Hovius, N.: Moisture Sources and Pathways Determine Stable Isotope Signature of Himalayan Waters in Nepal, AGU Adv., 4, 1–19, https://doi.org/10.1029/2022av000735, 2023.

He, S., Richards, K.: Stable isotopes in monsoon precipitation and water vapour in Nagqu, Tibet, and their implications for monsoon moisture, J. Hydrol., 540, 615–622, https://doi.org/10.1016/j.jhydrol.2016.06.046, 2016.

Hersbach, H., Bell, B., Berrisford, P., Hirahara, S., Horányi, A., Muñoz-Sabater, J., Nicolas, J., Peubey, C., Radu, R., Schepers, D.: The ERA5 global reanalysis, Q. J. R. Meteorol. Soc. 146, 1999–2049, https://doi.org/10.1002/qj.3803, 2020

Hoffmann, G., Cuntz, M., Jouzel, J., Werner, M.: A systematic comparison between the IAEA/GNIP isotope network and the ECHAM 4 atmospheric general circulation model, Isot. Water Cycle Past, Present Futur. a Dev. Sci., 303–320, 2005.

Huffman, G.J., Bolvin, D., Braithwaite, D., Hsu, K., Joyce, R., Kidd, C., Nelkin, E.J., Sorooshian, S., Tan, J., Xie, P.: Algorithm Theoretical Basis Document (ATBD) of Integrated Multi-satellitE Retrievals for GPM (IMERG), version 4.6. Nasa 29, 2017.

Jackisch, D., Yeo, B.X., Switzer, A.D., He, S., Cantarero, D.L.M., Siringan, F.P., Goodkin, N.F.: Precipitation stable isotopic signatures of tropical cyclones in Metropolitan Manila, Philippines, show significant negative isotopic excursions, Nat. Hazards Earth Syst. Sci., 22, 213–226, https://doi.org/10.5194/nhess-22-213-2022, 2022.

Kendall, C., Caldwell, E.A.: Fundamentals of Isotope Geochemistry, Isot. Tracers Catchment Hydrol., 51–86, https://doi.org/10.1016/B978-0-444-81546-0.50009-4, 1998.

Kleist, D.T., Parrish, D.F., Derber, J.C., Treadon, R., Wu, W.-S., Lord, S.: Introduction of the GSI into the NCEP global data assimilation system, Weather Forecast., 24, 1691–1705, https://doi.org/10.1175/2009waf2222201.1, 2009.

Knapp, K.R., Kruk, M.C., Levinson, D.H., Diamond, H.J., Neumann, C.J.: The international best track archive for climate stewardship (IBTrACS) unifying tropical cyclone data, Bull. Am. Meteorol. Soc., 91, 363–376, https://doi.org/10.1175/2009bams2755.1, 2010.

Krishnamurthy, V., Shukla, J.: Intraseasonal and seasonally persisting patterns of Indian monsoon rainfall, J. Clim., 20, 3–20, https://doi.org/10.1175/jcli3981.1, 2007.

Kurita, N.: Water isotopic variability in response to mesoscale convective system over the tropical ocean, J. Geophys. Res. Atmos., 118, 10,376-10,390, https://doi.org/10.1002/jgrd.50754, 2013.

Kurita, N., Noone, D., Risi, C., Schmidt, G.A., Yamada, H., Yoneyama, K.: Intraseasonal isotopic variation associated with the Madden-Julian Oscillation, J. Geophys. Res. Atmos., 116, 1–20, https://doi.org/10.1029/2010JD015209, 2011.

Lawrence, J.R., Gedzelman, S.D., Dexheimer, D., Cho, H.K., Carrie, G.D., Gasparini, R., Anderson, C.R., Bowman, K.P., Biggerstaff, M.I.: Stable isotopic composition of water vapor in the tropics, J. Geophys. Res. Atmos., 109 (D6), https://doi.org/10.1029/2003jd004046, 2004.

Lawrence, J.R., Gedzelman, S.D., Gamache, J., Black, M.: Stable isotope ratios: hurricane Olivia, J. Atmos. Chem., 41, 67–82, 2002.

Lawrence, J.R., Gedzelman, S.D., Zhang, X., Arnold, R.: Stable isotope ratios of rain and vapor in 1995 hurricanes, J. Geophys. Res. Atmos., 103, 11381–11400, https://doi.org/10.1029/97jd03627, 1998.

Lawrence, R.J., Gedzelman, D.S.: Low stable isotope ratios of tropical cyclone rains, Geophys. Res. Lett., 23, 527–530, https://doi.org/10.1029/96gl00425,1996.

Lekshmy, P.R., Midhun, M., Ramesh, R.: Role of moisture transport from Western Pacific region on water vapor isotopes over the Bay of Bengal, Atmos. Res., 265, 105895, https://doi.org/10.1016/j.atmosres.2021.105895, 2022.

Lekshmy, P.R., Midhun, M., Ramesh, R.: Spatial variation of amount effect over peninsular India and Sri Lanka: Role of seasonality, Geophys. Res. Lett., 42(13), 5500–5507, https://doi.org/10.1002/2015GL064517, 2015.

Lekshmy, P.R., Midhun, M., Ramesh, R., Jani, R.A.: ^{18}O depletion in monsoon rain relates to large scale organized convection rather than the amount of rainfall, Sci. Rep., 4, 1–5. https://doi.org/10.1038/srep05661, 2014.

Li, L., Chakraborty, P.: Slower decay of landfalling hurricanes in a warming world, Nature 587, 230–234, https://doi.org/10.1038/s41586-020-2867-7, 2020.

Li, Z., Yu, W., Li, T., Murty, V.S.N., Tangang, F.: Bimodal character of cyclone climatology in the Bay of Bengal modulated by monsoon seasonal cycle, J. Clim., 26 (3), 1033–1046, https://doi.org/10.1175/jcli-d-11-00627.1, 2013.

Liebmann, B., Smith, C.A.: Description of a complete (interpolated) outgoing longwave radiation dataset, Bull. Am. Meteorol. Soc., 77, 1275–1277, 1996.

Liu, Z., Tian, L., Yao, T., Yu, W.: Seasonal deuterium excess in Nagqu precipitation: Influence of moisture transport and recycling in the middle of Tibetan Plateau, Environ. Geol., 55, 1501–1506, https://doi.org/10.1007/s00254-007-1100-4, 2008.

Midhun, M., Lekshmy, P.R., Ramesh, R.: Hydrogen and oxygen isotopic compositions of water vapor over the Bay of Bengal during monsoon, Geophys. Res. Lett., 40, 6324–6328, https://doi.org/10.1002/2013GL058181, 2013.

Midhun, M., Pr, L., Ramesh, R., Yoshimura, K., Kk, S.: The effect of monsoon circulation on the stable isotopic composition of rainfall, J. Geophys. Res. Atmos., 123, 5205-5221, https://doi.org/10.1029/2017JD027427, 2018.

Mohapatra, M., Srivastava, A.K., Balachandran, S., Geetha, B.: Inter-annual variation and trends in Tropical Cyclones and Monsoon Depressions over the North Indian Ocean. Observed Climate Variability and Change over the Indian Region, Springer Geology, 89–106, https://doi.org/ 10.1007/978-981-10-2531-0_6, 2016.

Munksgaard, N.C., Zwart, C., Kurita, N., Bass, A., Nott, J., Bird, M.I.: Stable isotope anatomy of tropical cyclone ita, North-Eastern Australia, April 2014, PLoS One 10, 1–15, https://doi.org/10.1371/journal.pone.0119728, 2015.

Noone, D.: Pairing measurements of the water vapor isotope ratio with humidity to deduce atmospheric moistening and dehydration in the tropical midtroposphere, J. Clim., 25, 4476–4494, https://doi.org/10.1175/JCLI-D-11-00582.1, 2012.

Pandya, U., Khandelval, S., Sanghvi, H., Joshi, E., Vekaria, G.L., Jaaffrey, S.N.A., Soni, M.: Cyclone ‘TAUKTAE’-Observed through data & satellite images, 2021.

Paul, S., Chowdhury, S.: Investigation of the character and impact of tropical cyclone Yaas: a study over coastal districts of West Bengal, India, Saf. Extrem. Environ., 3, 219–235, https://doi.org/10.1007/s42797-021-00044-y, 2021.

Payne, V.H., Noone, D., Dudhia, A., Piccolo, C., Grainger, R.G.: Global satellite measurements of HDO and implications for understanding the transport of water vapour into the stratosphere, Q. J. R. Meteorol. Soc., 133, 1459–1471, https://doi.org/10.1002/qj, 2007.

Pfahl, S., Sodemann, H.: What controls deuterium excess in global precipitation? Clim. Past, 10, 771–781, https://doi.org/10.5194/cp-10-771-2014, 2014..

Rahul, P., Ghosh, P., Bhattacharya, S.K., Yoshimura, K.: Controlling factors of rainwater and water vapor isotopes at Bangalore, India: Constraints from observations in 2013 Indian monsoon, J. Geophys. Res., 121, 13,936-13,952, https://doi.org/10.1002/2016JD025352, 2016.

Rajeev, A., Mishra, V.: Observational evidence of increasing compound tropical cyclone-moist heat extremes in India, Earth’s Futur., 10, e2022EF002992, https://doi.org/10.1029/2022ef002992, 2022.

Risi, C., Bony, S., Vimeux, F.: Influence of convective processes on the isotopic composition ($\delta^{18}O$ and δD) of precipitation and water vapor in the tropics: 2. Physical interpretation of the amount effect, J. Geophys. Res. Atmos., 113, 1–12, https://doi.org/10.1029/2008JD009943, 2008.

Sánchez-Murillo, R., Durán-Quesada, A.M., Esquivel-Hernández, G., Rojas-Cantillano, D., Birkel, C., Welsh, K., Sánchez-Llull, M., Alonso-Hernández, C.M., Tetzlaff, D., Soulsby, C., Boll, J., Kurita, N., Cobb, K.M.: Deciphering key processes controlling rainfall isotopic variability during extreme tropical cyclones, Nat. Commun., 10, 1–10, https://doi.org/10.1038/s41467-019-12062-3, 2019.

Saranya, P., Krishan, G., Rao, M.S., Kumar, S., Kumar, B.: Controls on water vapor isotopes over Roorkee, India: Impact of convective activities and depression systems, J. Hydrol., 557, 679–687, https://doi.org/10.1016/j.jhydrol.2017.12.061, 2017.

Singh, A., Jani, R.A., Ramesh, R.: Spatiotemporal variations of the $\delta^{18}O$–salinity relation in the northern Indian Ocean, Deep Sea Res., Part I 57 (11), 1422–1431, https://doi.org/10.1016/j.dsr.2010.08.002, 2010.

Steen-Larsen, H.C., Sveinbjörnsdottir, A.E., Peters, A.J., Masson-Delmotte, V., Guishard, M.P., Hsiao, G., Jouzel, J., Noone, D., Warren, J.K., White, J.W.C.: Climatic controls on water vapor deuterium excess in the marine boundary layer of the North Atlantic based on 500 days of in situ, continuous measurements, Atmos. Chem. Phys., 14, 7741–7756, https://doi.org/10.5194/acp-14-7741-2014, 2014.

Sun, C., Tian, L., Shanahan, T.M., Partin, J.W., Gao, Y., Piatrunia, N., Banner, J.: Isotopic variability in tropical cyclone precipitation is controlled by Rayleigh distillation and cloud microphysics, Commun. Earth Environ., 3, https://doi.org/10.1038/s43247-022-00381-1, 2022.

Tian, L., Masson-Delmotte, V., Stievenard, M., Yao, T., Jouzel, J.: Tibetan Plateau summer monsoon northward extent revealed by measurements of water stable isotopes, J. Geophys. Res., 106, 28081–28088, https://doi.org/10.1029/2001JD900186, 2001.

Tian, L., Yu, W., Schuster, P.F., Wen, R., Cai, Z., Wang, D., Shao, L., Cui, J., Guo, X.: Control of seasonal water vapor isotope variations at Lhasa, southern Tibetan Plateau, J. Hydrol., 580, 124237, https://doi.org/10.1016/j.jhydrol.2019.124237, 2020.

Tian, L., Yao, T., Numaguti, A., Sun, W.: Stable isotope variations in monsoon precipitation on the Tibetan Plateau, J. Meteorol. Soc. Japan., 79, 959–966, https://doi.org/10.2151/jmsj.79.959, 2001.

Uemura, R., Matsui, Y., Yoshimura, K., Motoyama, H., Yoshida, N.: Evidence of deuterium excess in water vapor as an indicator of ocean surface conditions, J. Geophys. Res. Atmos., 113, https://doi.org/10.1029/2008jd010209, 2008.

Verma, K., Gupta, A., 2021. Cyclone Tauktae: Cyclones, Their Impacts and Disasters Risk Management.

Villarini, G., Smith, J.A., Baeck, M.L., Marchok, T., Vecchi, G.A.: Characterization of rainfall distribution and flooding associated with US landfalling tropical cyclones: Analyses of Hurricanes Frances, Ivan, and Jeanne (2004), J. Geophys. Res. Atmos., 116, https://doi.org /10.1029/2011jd016175, 2011.

Wei, Z., Yoshimura, K., Okazaki, A., Ono, K., Kim, W., Yokoi, M., Lai, C.T.: Understanding the variability of water isotopologues in near-surface atmospheric moisture over a humid subtropical rice paddy in Tsukuba, Japan, J. Hydrol., 533, 91–102, https://doi.org/10.1016/j.jhydrol.2015.11.044, 2016.

Worden, J., Noone, D., Bowman, K.: Importance of rain evaporation and continental convection in the tropical water cycle, Nature, 445, 528–532, https://doi.org /10.1038/nature05508, 2007.

Xu, T., Sun, X., Hong, H., Wang, X., Cui, M., Lei, G., Gao, L., Liu, J., Lone, M.A., Jiang, X.: Stable isotope ratios of typhoon rains in Fuzhou, Southeast China, during 2013–2017. J. Hydrol., 570, 445–453, https://doi.org/10.1016/j.jhydrol.2019.01.017, 2019.

Yoshimura, K.: Stable Water Isotopes in Climatology, Meteorology, and Hydrology: A Review, J. Meteorol. Soc. Japan, 93, 513–533, https://doi.org/10.2151/jmsj.2015-036, 2015.

Yu, W., Yao, T., Tian, L., Ma, Y., Ichiyanagi, K., Wang, Y., Sun, W.: Relationships between $\delta^{18}O$ in precipitation and air temperature and moisture origin on a south-north transect of the Tibetan Plateau, Atmos. Res., 87, 158–169, https://doi.org/10.1016/j.atmosres.2007.08.004, 2008.